UNIVERSIDADE TÉCNICA DE LISBOA

INSTITUTO SUPERIOR TÉCNICO

MODELLING OF ARSENIC DYNAMICS IN THE TAGUS ESTUARY

Luís Daniel Fachada Fernandes

(Licenciado)

Dissertação para obtenção do grau de Mestre em

Ecologia, Gestão e Modelação dos Recursos Marinhos

Orientador:	Doutor Ramiro Joaquim de Jesus Neves
Co-orientador:	Doutor Paulo Miguel Chambel Filipe Lopes Teles Leitão
Presidente:	Doutor Ramiro Joaquim de Jesus Neves
Vogais:	Doutor Flávio Augusto Bastos da Cruz Martins
	Doutor Aires José Pinto dos Santos
	Doutor Paulo Miguel Chambel Filipe Lopes Teles Leitão

Março de 2005

Título	Modelação da Dinâmica do Arsénio no Estuário do Tejo
Nome	Luís Daniel Fachada Fernandes
Mestrado em	Mestrado em Ecologia, Gestão e Modelação dos Recursos Marinhos
Orientador	Ramiro Joaquim de Jesus Neves
Co-orientador	Paulo Miguel Chambel Filipe Lopes Leitão
Provas concluídas em	29 de Junho de 2005

Sumário

Um modelo numérico de transporte de contaminantes foi desenvolvido no sistema de modelação MOHID, utilizando uma filosofia de programação orientada por objectos. O modelo encontra-se dividido em dois compartimentos principais: a coluna de água e o leito de sedimentos, que comunicam entre si através duma interface sedimento-água. Na coluna de água, o transporte das fases particuladas e dissolvidas dos contaminantes é calculado recorrendo a um módulo hidrodinâmico. Processos, tais como adsorpção/desorpção aos sedimentos, tanto em suspensão como no leito; erosão/deposição de sedimentos contaminados; transporte na água intersticial; efeitos da bioturbação nas propriedades dos sedimentos; e fluxos na interface sedimento-água, encontram-se incluídos no modelo.

O modelo foi utilizado como ferramenta para um estudo integrado do transporte, e destino final do arsénio, no estuário do Tejo. O modelo tenta compreender os efeitos de várias décadas de descargas de arsénio no estuário do Tejo, pela unidade industrial de processamento de arsenopirite no Barreiro; simular o seu transporte e distribuição e ainda determinar as zonas mais contaminadas pela descarga.

Palavras-chave: modelo, contaminantes, programação orientada por objectos, arsénio, estuário do Tejo, MOHID

Title Modelling of Arsenic Dynamics in the Tagus Estuary

Abstract

A numerical estuarine contaminant transport model was developed in the framework of MOHID Water Modelling System, using an object oriented approach. The model is divided into two major compartments: the water column and the sediment column, that communicate through a sediment-water interface. In the water column, the particulate and dissolved phases transport is computed by coupling a transport module with a hydrodynamic model. Processes such as adsorption/desorption on to sediments, both in suspension and in the deposited bed; erosion/deposition of contaminated sediments; transport in sediment porewater; bioturbation effects on sediments; and fluxes at the water-sediment interface are simulated.

The model was used to perform an integrated study of arsenic transport and fate in the Tagus estuary. The model attempts to reproduce several decade discharges of arsenic into the Tagus estuary performed by the Quimigal arsenopyrite processing plant in the Barreiro industrial zone and to simulate its transport and distribution, as well as acknowledge the most contaminated zones, comparing the results with several measurements taken contemporarily with the discharge.

Keywords: model, contaminants, object-oriented programming, arsenic, Tagus estuary, MOHID

Acknowledgements

I would like to thank Prof. Ramiro Neves for giving me the opportunity to carry out this work, and for its guidance and availability through these last couple of years I have been working with him.

I would like to thank Prof. Alexandre Bettencourt for the field data availability, for his important remarks and also for his determination to work in this modelling study.

I would also like to wish my sincere thanks to all my colleagues and friends at MARETEC and HIDROMOD, for the dynamic spirit and motivation to reach high in research and modelling. This work would never be possible without your help. I would especially like to thank Paulo Chambel Leitão for his dedication, support and teamwork, for his knowledge and fruitful discussions; to Frank Braunschweig for all the things I have learned from him and for all the brainstorming during the model restructure; to Pedro Chambel Leitão who has walked with me in the despairing times of the first attempt to connect the sediment module, for his patience and friendship, to Pedro Pina, who started this work and is always a reference to me. To Guillaume Riflet, for his work on the MOHID vertical 1D mode, that proved to be very useful in the calibration of the contaminant transport model.

To all of those who have contributed, and continue to contribute in MOHIDs' project and to all my friends and colleagues who, optimistically, have pushed me into to pursuing this gold.

A special thanks to Sofia for everything, for your encouragement, support and balance.

To my family, especially to my parents, who have always unconditionally supported and encouraged me, I thank you.

Finally, I would like to thank the financial support provided by the FCT, in the framework of the MOBIDYCS project, ref. POCTI/BSE/33735/99.

INDEX

FIGURES INDEX

TABLE INDEX

1 INTRODUCTION

1.1. Overview

Many estuarine systems are and have been subjected to chronicle contamination, due to continuous domestic, industrial and diffuse pollutant discharges. This type of contamination does not always presents visible effects, but, because it is so spread and it occurs in a regular way, it can, on a global basis and in a longer time scale, be more important than other pollution events, more visible and with more restricted mortality. An indispensable requirement to mitigate estuarine pollution effects is the ability to understand and predict the distribution, transport and fate of contaminants. Numerical models can, in this field, represent an important role as a decision support tool in water quality management. The development of these numerical tools and its application to coastal areas and estuaries, results on a multidisciplinary study of these complex environmental systems and, consequently, on the definition of the most important processes and parameters that influence contaminant dynamics.

Contaminants, being heavy metals, metalloids, pesticides or hydrocarbons, occur generally in the aquatic environment in two distinct forms: dissolved or adsorbed on to particulate matter. It is largely recognized the importance of the adsorbed phase because of the relevant fraction it represents in the global distribution of the contaminant. Thus, the transport and

fate of particulate matter must be well known if one aspires to describe the paths of an important fraction of the contaminant. This fraction can be mostly related with the fine fraction of the particulate matter, the cohesive sediments. Cohesive sediments tend to settle on the bottom of the aquatic systems, where they can stay and be buried by other settling sediments, or they can be resuspended back to the water column. It is important to define cohesive sediment deposition zones because it is where contaminated sediments tend to deposit and stay, resulting in the imprisonment and concentration of the contaminant and its consequent removal from the water column. But removing it from the water column, does not mean that the contaminant exits the system, because when remaining in the sediments it can be subjected to a series of processes that can result on its remobilisation or/and affect the benthic habitats. This way, these deposition zones can be, through years of pollutant discharges, more disposed to be affected.

1.2. Objectives

The object of this dissertation is to present an integrated study of arsenic transport and fate in the Tagus estuary. A numerical contaminant transport model was developed using state-of-the-art object oriented programming techniques, in order to merge the interdisciplinary approach that such a study requires. The model attempts to simulate several decade discharges of arsenic into the Tagus estuary performed by the Quimigal arsenopyrite processing plant in the Barreiro industrial zone and to simulate its transport and distribution; acknowledge the most contaminated zones, comparing the results with several measurements taken contemporarily with the discharge. The aim of this thesis is to describe the governing processes in contaminant transport and fate and to describe the tools and hypothesis used to design the model, as well as contribute with a useful numerical tool that can be applied both in scientific studies and in decision making.

1.3. Organization

This document will be divided into 6 different chapters. The following chapter will describe contaminant transport processes in estuaries such as hydrodynamics, adsorption-desorption, cohesive sediments, consolidation, bioturbation and diagenesis. On the third chapter, a review on contaminant transport models is presented and a comparison is made, in terms of

processes included in the software, relatively to the MOHID, the model used and developed in the framework of this study. Further in this chapter, the developed contaminant transport model is presented in terms of implementation, structuring and design, and processes equations. Model calibration is then presented on chapter four, where some test cases are performed to verify the consistency of the model. Model results of an application to the Tagus estuary are presented in chapter five, where different methodologies are used and comparisons with measurements are made. A discussion on results is also included. The final chapter reviews all the main features of this thesis and discusses key conclusions and future work.

2 CONTAMINANT TRANSPORT IN ESTUARIES

2.1. Introduction

Estuaries are extremely dynamic systems, that move and change constantly in response to winds, tides and river fresh water inputs. Hence, comprehending the transport and fate of pollutants in these systems, requires the knowledge of the physical, chemical and biological processes that occur there, as well as the contaminants properties themselves.

The terms contaminant and pollutant can be described separately but are often in effect synonymous. Both are used to describe chemicals that are found at levels judged to be above those that would normally be expected (Walker et al, 1996). Contamination can be defined as any artificial increase above background level; and pollution, implies harm to living things. This is not a distinction made in the dictionary, nor is it universally accepted by ecologists (Taylor, 1993 in James, 2002). Whether or not a contaminant is a pollutant may depend on its concentration in the environment and on the organism or system being

considered; thus, one particular substance may be a contaminant relative to one species but pollutant relative to another. Finally, in practice, it is often difficult to demonstrate that harm is not being caused, so that in effect, pollutant and contaminant become synonymous (Walker et al, 1996).

Thus, a pollutant may be defined as any substance that reduces the water quality. It may or may not result from human activity. It may have a well-defined source (such as an oil spill) or a diffuse source (e.g. radioactivity from the atmosphere, antifouling paints) (James, 2002).

In a cyclic perspective, a contaminant, entering an estuary by local or diffuse source, is controlled by the hydrodynamics, resulting from sea and river encounter, and can be distributed, according to environmental conditions, into two phases: dissolved and adsorbed. The adsorbed, or particulate, phase is associated with particles in suspension, therefore being the sediment bed its main final location. If resuspended, it can be remobilised to the water column. The dissolved phase, flows in the estuary, depending on the equilibrium with the particulate phase and on contributions from the sediment bed porewater, due to the concentration of pollutants there. Finally, it can be exported to the ocean.

A great deal of processes must be studied in order to perform an integrated study such as contaminant transport in estuaries. Models are recognized to be powerful tools that enable the study and integration of variables controlling the distribution, in time and space of pollutants, thus making possible to estimate and predict their path along an estuarine system. Consequently, they become useful in many purposes, such as: aiding experimental design; linking cause and effect; designing scenarios for hypothetical situations; or just predict contaminant path and evolution in time and space (Pina, 2001).

2.2. Processes controlling the transport and fate of contaminants in estuaries

2.2.1. Hydrodynamics and transport

Hydrodynamics is the driving force in the transport of chemical (pollutants, nutrients), biological (plankton) and geological (sediments) substances in an estuary. In estuaries, in general, tide and density gradient effects are the governing processes controlling hydrodynamics, which combined with bottom shear, atmospheric forcing (wind, solar radiation, etc) and topographic variation, result in a highly complex non-linear system. Contaminants inside an estuary are subjected to transport in the water column by hydrodynamic currents. These currents can be characterized by a turbulent flow presenting chaotic behaved fluctuations in time and space, characterized by complex vortexes structures.

2.2.2. Adsorption-Desorption

Adsorption relates to the process where a solute in a liquid phase becomes bonded to the surface of a solid (Linde, 2002). It can occur in three major pathways: physical adsorption, electrostatic adsorption and specific adsorption.

Desorption, the opposite process of adsorption, is likely to depend on salinity, as metals may be released from particles as they traverse the salinity gradient and encounter dissolved seawater ions, which compete for sorption sites or complex favourably with sorbed metals. Changes in pH and redox conditions, bacterial or chemical degradation of particulate organic matter (Martino et al, 2002) can also be accounted for desorption.

In some cases precipitation and dissolution can be compared as adsorption and desorption, respectively. They are different processes but with some similar practical results, removing a constituent from the dissolved phase. Precipitation is called to the process solid formation from the combination of two or more solutes. A subset of precipitation is chemical substitution, or co-precipitation, when a separate trace element becomes included in the crystal structure of the precipitating solid (Linde, 2002).

One way to parameterise the distribution of a constituent in the aquatic environment is by determination of the ratio between the adsorbed particulate concentration and the dissolved concentration. This ratio is a general approach in contaminant transport modelling (Johansson et al., 2001; James, 2002), and is known as the partition coefficient.

Physically, the partition coefficient, as widely described by literature (Johansson et al., 2001), illustrates particle affinity and represents the chemical equilibrium of numerous processes such as sorption onto particulate matter, precipitation and dissolution.

This model can be applied to trace elements, as the limitation of adsorption sites in particulate matter, relatively to the low metal concentrations, can be considered not to be critical. Depending on the reversibility of these processes the partition coefficient should not be regarded as a constant but rather as a variable (Johansson et al., 2001). Again literature widely describes the factors influencing the equilibrium as being, for example, pH, salinity, concentration of suspended particulate matter, redox conditions, biogenic silica and concentration of dissolved organic matter. Examples of substances for which the partition coefficient has been either determined or modelled are: trace metals, organic micro pollutants, phosphorus and radionuclides (Johansson et al, 2001).

2.2.3. Cohesive sediment transport in estuaries

2.2.3.1. General overview

Pollutants transport in the adsorbed phase is strongly connected with cohesive sediment transport due to the affinity of many contaminants for the solid phase. Once adsorbed to the sediments, these substances are transported by the sediments, being their fate controlled by the dynamic of the latter in the estuary.

Estuarine suspended particles are derived from continental and coastal erosion, in situ chemical and biological processes, the atmosphere, and industrial activities. Their composition can be broadly categorized into four components (Turner & Millward, 2002):

- a lithogenous component, which is inorganic material derived from the weathering of crustal material and is mainly composed of quartz and other primary silicate minerals such as feldspar, and secondary silicate minerals (clays);

- a hydrogenous component is generated in situ by chemical processes, and exists either as coatings on lithogenous material, or as discrete phases. Hydrogenous phases include iron and manganese oxides, carbonates, sulphides and humic aggregates;

- a biogenic component is generated in situ or externally by biological processes, and includes micro organisms (bacteria, fungi, protozoan), plankton, decaying remains of organisms, faecal matter and marine and terrestrial plant debris, or, from a biochemical standpoint, proteins, carbohydrates, lipids and pigments.

- an anthropogenic component includes sewage solids, plastics, tar, solvents, surfactants, mine tailings, coal dust and fly ash, and may occur as discrete particles, or as non-aqueous phase liquids adhered to or entrapped within the particle matrix biogenic entities (or seston), may be conceptualized as follows.

2.2.3.2. Hydrodynamics

Hydrodynamics is the most important mechanism involved in the estuarine cohesive sediment transport providing the advective component, generating the turbulence responsible for eroding the sediment deposits and for playing an important role in particulate matter flocculation (Cancino & Neves, 1999a). Generally, tidal currents and waves dominate the local estuarine hydrodynamics, thus determining the physical, morphological and biological characteristics of a mud-flat (Christie et al, 1999).

In tidal flows, the horizontal transport is mainly advective, and is induced by the propagation of the tide into the estuary, heavily depending on its geometry. Times of high and low water will be increasingly retarded upstream the estuary and the tidal wave will distort, resulting in a flood- or ebb- dominated tidal regime. Slack water periods allow sediments to deposit, while during high current periods the bottom is eroded. The time lag between both periods and the relative strength of the ebb/flood currents will determine in which direction residual horizontal transport will take place (deClippele, 1998).

Estuarine local waves can produce bottom shear stress and therefore can also play an important role as they act as a destabilization, mobilization and suspension factor for sediments and a minimal current may be able to carry away the already activated sediment grains.

2.2.3.3. Flocculation

The aggregation of suspended particles in flocks is essential for sedimentation, as larger flocks, in addition to enhance sedimentation, enable it in the first place (van der Lee, 2001). The probability of particles to aggregate depends on the probability of them to collide (Cancino & Neves, 1999a) and on collision efficiency. Collision of particles depends essentially on the concentration of particles in suspension, on turbulence, on their approach due to Brownian movements and on the fact that they have different settling velocities. Brownian movements and differential settling can be considered negligible in terms of transport in estuaries and coastal waters (Winterwerp, 2002), due to the flow turbulent characteristics. The efficiency of collision depends on particles characteristics (e.g. organic matter content, biological source) and on environmental conditions, where salinity plays an important role.

Sediment particles have a relatively inert core, comprising primary and secondary silicates, which is surrounded by a more reactive coating, comprising iron and manganese oxides, carbonates, sulphides, detrital organic matter and micro organisms. They are enveloped in a film of organic matter which provides a net negative charge to the surface (Turner & Millward, 2002**).** This negative charge is counterbalanced by a cloud of positive ions formed around them, which forms a double electric layer. When two particles approach, electrostatic repulsion avoids their collision. Salinity causes the thickness of the double electric layer to diminish due to the lower gradient between the concentration of positive ions around the particle and ions concentration in water. Thus, particles can come close enough so that van der Waals forces become stronger than the electrostatic repulsion, therefore occurring flocculation.

The particle aggregates present different characteristics in relation to individual particles. Their dimension can reach several orders of magnitude higher (e.g. millimetres); they are fragile and tend to break; their specific mass is smaller due to the interstitial water present in their constitution; their shape is rounder or spherical relatively to the more laminar shape of a single particle, which reduces its resistance.

2.2.3.4. Settling velocity

The settling velocity of a particle in a fluid depends on gravitational forces - which, in turn, depends on the density of each individual particle and on the interstitial water volume existing in the flocks formed by particles – and on shear produced by the settling movement – that depends on the shape of the flock and on the Reynolds number around the flock during settling (Cancino & Neves, 1999a).

Particle concentration is an important and dominant mechanism in the settling process. When their concentration becomes high enough, the settling flocks start to hinder each other in their movements, a process generally known as hindered settling (Winterwerp, 2002), and represents the diminishing of the settling velocity.

2.2.3.5. Deposition

High bed stresses caused by flow and waves exerted by peak tidal flows, constitute a barrier to deposition. Krone(1962) proposed the concept of a limiting value for shear stress, above which no deposition takes place. This hypothesis is the most used in deposition models in numerical cohesive sediment transport models. However, most models consider deposition and erosion never to occur at the same time. deClippele (1998) encountered in literature values varying from 0.06-0.5 Pa, mainly obtained from laboratory experiments. The rate of mud deposition onto the bed or deposition flux, is the product of the potential settling flux from the lowest layer and the probability of it sticking to the bed. This concept reflects the fact that the flock deposition is controlled by near-bed turbulence or, more specifically, by the rate of near-bed shearing. The critical shear stress for deposition depends mainly on the size of the flocks. Larger flocks present a higher probability to remain in the sediment bed than smaller flocks (Cancino & Neves, 1999a).

2.2.3.6. Erosion

The possibility of a sediment bed to be eroded is conditioned by the shear stress near the bed and by its cohesive properties, which conversely depends on clay mineralogy and on biogeochemical processes. Erosion of cohesive sediment has generally been observed to occur in one of two modes: particle by particle or mass erosion. The first corresponds to the case in which particles separate from the bed on an individual basis, as a result of hydrodynamic forces exceeding cohesive bonding, frictional and gravitational forces; in the

latter case, portions of the bed become unstable and large masses of sediment are resuspended. Particle by particle erosion is, however, the most common erosion mechanism in estuaries; under the action of bottom shear stresses higher than the bed shear strength, removal of particles and decrease in bed elevation (scour) will advance until a bed layer of higher strength, equal to the applied stress, is found (deClippele, 1998). This increase in bed shear strength with depth is due to changes in the flock structure after deposition, during consolidation and gelling.

On the modelling perspective, similarly to the deposition process, one can consider that erosion occurs when shear stress near the bottom exceeds a certain threshold value representative of the bed effective strength. This threshold value depends on the consolidation, which depends on the age of the deposit; and particle adhesion, which depends namely on clay and organic matter content, where biological processes play an important role. In intertidal zones, some other processes can influence erosion. Low tide exposure allows drying of the surface sediment, through evaporation by sunlight and wind. Amos et al (1988) (in Christie et al, 1999) show drying can increase the critical shear stress of sediment, thus inhibiting erosion. Heavy rainfall may reverse this process and reduce it.

Houwing (1999) presents a case study on the determination of the critical erosion threshold on mud flats. He found no clear relationship between distinct parameters like bed density, moisture content or biological activity and the critical erosion threshold, and presents a review of erosion characteristics such as critical erosion shear stress values varying between 0.02 N/m^2 for fluff layer top and 0.7 N/m^2 for air exposed mud. This states the level of uncertainty and the difficulty to parameterise such coefficients in a cohesive transport models. Regarding the erosion rates, Houwing (1999) presents values varying in two orders of magnitude (10^{-3}-10^{-5} kg/m^2s^{-1}), a fact that corroborates this difficulty.

2.2.3.7. Consolidation

For high concentration suspensions, the transition between the water column and the sediment bed can be made through a dense suspension, normally known as fluid mud, which depending on its concentration can be mobile or stationary. The formation of this layer is related to the fact that the deposition rate is sometimes higher than the consolidation rate or due to the fluidization of the bed by influence of the turbulent water flow near the bed. For low concentrations, sediments easily deposit directly on the bed,

forming a structure where density and shear strength can increase rapidly in depth. Consolidation can be described as the decrease in sediment bed volume resulting from dissipation of excess pore pressure, consisting basically on the formation of structures, or sediments aggregation, gradually becoming denser. This causes interstitial waters to be expelled. This process can be characterized by the collapse of particles to an interstice occupied by water, which initially supported its weight, causing it to be expelled upwards. Consolidation occurs when interstitial pressure is higher than hydrostatic pressure, due to the weight of solid particles above and higher than the shear forces produced by flow through porous media and shear between sediment particles. Consolidation stops when these forces balance each other.

This can be an important process in contaminant transport by the fact that it influences the erosion rates, consequently affecting contaminant remobilisation to the water column, and it affects contaminant transport inside the sediment bed, both by porewater flow and changing the properties of the bed.

2.2.4. Bioturbation

Benthic organisms' biological activity has a significant importance in fluxes between the sediment and the water column. This activity can enhance mixture, affecting diffusion processes in the upper layers of the sediment bed, as well as intervene in the erosion and deposition processes by altering sediment properties (porosity, cohesion, rugosity) at the interface.

These organisms cause perturbations in the sediments mainly due to its movement in search for food and shelter from their predators (Boudreau, 1997), modifying the micro-topography of the sediment bed and creating biogenic structures through the aggregation of flocks (some species include in their faeces digestion remains that contain cohesive properties); forming pathways; building various types of wells, tubes, tunnels (i.e. bio-irrigation); small excavations (Graf and Rosenberg, 1997).

Riedel et al (1997), in experiments with contaminated sediments with arsenic, verified that the excavation activities of the polychaete *Nereis succinea* enhanced in a factor of five the arsenic fluxes at the sediment-water interface. In an extension of those experiments it was

detected that this influence depended, beside the type of fauna, in the food intake behaviour and type of activity.

2.2.5. Diagenesis

The geological term that defines diagenesis refers to the process by which sediment, subsequently to its deposition, transforms into sedimentary rock.

Normally, some processes described above, such as consolidation and bioturbation, are included as part of diagenetic processes. In this text, it was decided to separately discuss these processes that occur in the sediments, namely the decomposition of organic matter and dissolved oxygen consumption in sediment porewater. Porewater is an important indicator of the sediment properties, as it functions as a vehicle for substances (e.g. nutrients, contaminants) and as media for reactions in the sediment compartment.

On the superficial layer of the sediment bed, organic matter decomposition by micro-organisms depletes dissolved oxygen concentration in the interstitial waters. If the oxygen diffusive flux from the surface is not enough to satisfy this depletion, micro-organisms start to consume nitrates, reducing them. Once nitrates are depleted, they rapidly pass to manganese and iron oxide sources and from there to sulphates, abundant in reduced environments. Decomposition is then mediated through sulphate reducing bacteria producing sulphide acid. As anoxic conditions are achieved, bacteria obtain energy through fermentation, producing methane.

Diagenetic processes regulate physical and chemical conditions of the sediments, resulting into vertical stratification, generally characterized by dissolved oxygen concentrations. Oxygen depletion in porewater reduces manganese and iron oxide releasing metals adsorbed to sediment, which on the other hand, are again remobilized to more oxygenated waters and even to the water column, increasing its availability.

Methane formation in the fermentation process can lead to its accumulation in bubbles in the sediment. These bubbles, when reaching a critical pressure might burst, causing an increase in mixing processes and in sediment resuspension to the water column, with all its implications.

3 CONTAMINANT TRANSPORT MODELLING

3.1. Coastal and estuarine contaminant transport models

There is, among the scientific modelling community, a high variety of contaminant transport models. These models cover a wide range of processes, complexity and application areas. Since the 1960's, when the first hydrodynamic models began to be developed, the computational demands have grown at approximately the same rate as computational power development. Thus, models have fully fledged to complex software systems integrating and covering a great deal of environmental processes. Therefore, when using a model as a scientific or engineering tool, one must be aware that the model, in order to produce reliable results, must be adjusted to the system in study and also to the type of processes to be explored.

As an example exercise, a list of coastal and estuarine waters contaminant transport models is presented and compared. Note that the models were chosen by their complexity, comparability, interdisciplinary approach and their versatility, and that the comparison terms are strictly restricted to the identification of processes and approaches included in

each model. WASP, SMS and CHEMMAP modelling systems are software packages including more than one model, thus, comparison is made taking into account that the included models can be considered as one complex model. Each of the selected models is identified by a number to which the reader shall address in Table 1 and Table 2. Note that MOHID, the model developed and applied in the framework of this thesis is placed in the right-most column of the referred tables.

1. **WASP** (Water Quality Analysis Simulation Program), Environmental Protection Agency, USA;
2. **SMS** (Surface Water Modelling System), Brigham Young University, USA;
3. **MIKE 3**, Danish Hydraulic Institute, Denmark;
4. **CHEMMAP** (Integrated Chemical Discharge Model System), Applied Science Associates, Inc, Narragansett, Rhode Island, USA;
5. **HSCTM2D** (Hydrodynamic, Sediment and Contaminant Transport Model), Multiple authors;
6. **DELFT3D**, Delft Hydraulics, The Netherlands
7. **MOHID** ("Modelo Hidrodinâmico" – Hydrodynamic Model), MARETEC, Instituto Superior Técnico, Technical University of Lisbon, Portugal

Model		1	2	3	4	5	6	7
Physical domains	Rivers	√	√	√	√	√	√	√
	Lakes/Reservoirs	-	√	√	√	√	√	√
	Coastal Waters/Estuaries	√	√	√	√	√	√	√
	Ocean	●	-	√	-	-	√	√
Freeware		√	●	●	-	√	●	√
Open source		√	●	●	-	√	●	√
Graphical user interface		√	√	√	√	●	√	√
Programming language		F77	-	F90	-	F77	F77	F95
Object oriented programming		●	-	●	-	●	●	√
Parallel processing		●	-	-	-	●	●	√
Spatial discretization	Method	-	FE/FD	FD	FD	FE	FD	FV
	Dimensions	1D	2D/3D	3D	3D	2D	3D	3D
	Boundary fitted grid	-	√	●	√	●	√	√
	Vertical coordinates	-	-	-	σ	-	σ / z	G

Table 1 - Global characteristics comparison for the selected contaminant transport models;

Spatial discretization: methods FE (finite elements), FD (finite differences), FV (finite volumes); Vertical coordinates: G (generic), σ (sigma), z (cartesian); Prog. Languages: F (FORTRAN)

(- corresponds to non available information)

Model		1	2	3	4	5	6	7
Hydrodynamic s	Database coupling	√	√	√	√	●	√	√
	Run-time	●	√	√	√	√	√	√
Cohesive sediments	Transport	√	√	√	√	√	√	√
	Waves influence	●	√	√	-	●	√	√
	Erosion	√	√	√	√	√	√	√
	Deposition	√	√	√	√	√	√	√
Non-cohesive sediments	Transport	●	√	√	-	●	√	√
	Waves influence	●	√	√	-	●	√	√
Sediment bed	Consolidation	√	●	√	-	●	√	√
	Porewater advection	●	●	-	-	●	√	√
	Particulate/dissolved phases	●	●	-	-	●	√	√
Contaminants	Transport	√	√	√	√	√	√	√
	Particulate/Dissolved phases	√	√	√	√	√	√	√
	Adsorption/Desorption	√	√	√	√	√	√	√
	Degradation	√	√	√	√			√
	Interaction with sediment bed	√	-	√	-	√	√	√
	Particle tracking	●	-	√	√	●	●	√
	Particle adsorption/desorption	●	-	-	√	●	●	√
	Particle erosion/deposition	●	-	-	√	●	●	√

Table 2 - Specific characteristics of the selected contaminant transport models (- corresponds to non available information)

Most contaminant transport models comprise hydrodynamics, 2D/3D transport, cohesive and non-cohesive transport, the concept of dissolved and particulate phases regulated by adsorption/desorption processes. These can be seen as the major processes governing contaminant transport and fate in estuaries, in a physical perspective. Biological and chemical activity, both in the pelagic and benthic environments, is also relevant. In the following pages, these processes will be described in more detail, with some attention being paid to bioturbation and to diagenetic processes.

3.2. Mohid Water Modelling System overview

This chapter comprises the description of the integrated numerical tool, MOHID Water, used and developed in the framework of this thesis. The underlying principles behind the global design of the model are presented, with special attention paid to the contaminant transport modelling features.

MOHID Water is a numerical model included in MOHID Water Modelling System (Braunschweig, 2004a, Braunschweig, 2004b), an integrated water modelling software system that can be used to simulate surface water bodies, porous media flow and infiltration, and watersheds.

3.2.1.1. Some history

MOHID Water is the latest version of MOHID long set of evolutions which started back in 1985. Since that time, a continuous development effort of new features has been maintained. Model updates and improvements were made available on a regular basis and were used in the framework of many research and engineering projects.

Initially, MOHID was a two-dimensional tidal model written in FORTRAN 77 (Neves, 1985). This version also gave the present name to the model, which derives from the Portuguese abbreviation of "*MOdelo HIDrodinâmico*" (Hydrodynamic Model). Traditionally known as a hydrodynamic model, it was used to study estuaries and coastal areas using a classic finite-differences approach. Further developments, included the conversion to 3D and addition of baroclinic effects (Santos, 1995) and full discretization to finite volumes approach to allow the use of generic vertical coordinates (Martins, 2000). Previous versions of the model have been applied in numerous studies and integrating a

wide variety of processes and scales. Below is an exemplificative list of some recent applications performed with MOHID:

- Estuaries: Sado estuary, Portugal (Martins et al, 2001); Tagus estuary, Portugal (Leitão, 2003; Braunschweig, 2003, Pina et al, 2004); Guadiana (Saraiva et al, 2004);
- Coastal lagoons: Ria de Aveiro (Leitão, 2003; Trancoso et al, 2005); Ria Formosa (Silva et al, 2002); Reservoirs: Roxo, Monte Novo and Alqueva reservoirs (Braunschweig, 2001);
- Coastal areas: Ria de Pontevedra (Villarreal, 2002); Ria de Vigo (Montero, 1999; Leitão, 2003)
- Oceans: European ocean margin (Santos et al, 2002), Iberian Coast (Coelho et al, 2002); Brazilian Coast (Leitão, 2003);

Several other applications are currently being developed in the framework of research and engineering projects. These applications comprise systems as small and complex as annular flumes (MOBIDYCS project); high resolution 3D simulations in the Oosterschelde, The Netherlands (MABENE); large systems like the North Sea with integrated hydrodynamic and ecological simulations (EUROTROPH, MABENE); or cohesive sediment transport over submarine canyons (EUROSTRATAFORM).

A substantial increase in the number of users has occurred since the model was made available on the internet (http://www.mohid.com) backed up by a user's online forum where discussion around the model takes place.

The model robustness in hydrodynamics, allowed the development and coupling of a transport model, including cohesive sediment transport (Cancino & Neves, 1999a). This development also allowed the coupling of a water quality (eutrophication) module (Portela, 1996; Miranda, 1999; Pina, 2001; INAG, 2002; Saraiva et al, 2004) that opened new frontiers for model applications and that transformed the model as a fully integrated tool, ready to be applied to almost every aquatic system. However, this development was not sustainable as the number of programmers and users increased, due to the interdisciplinary approach of the model, and the programming methodology was found not to be appropriate with the aspirations of the model. At some stage it began difficult to maintain and to extend due to

the FORTRAN 77 language limitations and due to the increasing number of users and programmers and the interdisciplinary character of the modelled processes. Thus, it was necessary to establish a methodology which permitted to reuse the code more often and improve its robustness related to programming errors (Leitão, 2003). It was decided to reorganize the model, writing it in ANSI FORTRAN 95, profiting from all its new features, including the ability to produce object oriented programming with it, although it is not an object oriented language. This migration began in 1998, implementing object oriented features like described in Decyk et al (1997) with significant changes in code organization (Miranda et al, 2000). This migration resulted in an object oriented model for surface water bodies which integrates different scales and processes (Leitão, 2003).

The object oriented strategy brought MOHID the penalty of increasing the execution time by two or three times (Miranda et al., 2000) and the number of code lines, but on opposite, it has proven to be very reliable and robust. Programming errors, which would manifest as program memory errors and were found with some regularity, have completely disappeared and other logical errors are more easily found, since this approach was adopted (Braunschweig, 2001). Thus, MOHID development has been a relatively straightforward task due to the use of this philosophy.

3.2.1.2. Coupling the contaminant transport model

A contaminant transport model in the water column was introduced in MOHID, in a straightforward way (EUROSSAM, 2000). However, has described before, the sediment bed can play an important role in contaminant transport and fate, therefore it was considered crucial to implement it in the model in a more comprehensive way. The first approach to couple a sediment compartment module to MOHID revealed to be complex, as the configuration and design of the model was not prepared to include such modification. Communication between modules was not clear, therefore difficult to perform, namely when computing fluxes through the water-sediment interface. In other words, it was difficult to change water and sediment properties in a reciprocate way, as the water column was not programmed to do so. The will to include a contaminant transport model in MOHID and the spreading evolution of the model into other application areas in water modelling (porous media flow, watershed modelling, etc), brought the necessity to reorganize its structure. MOHID was exclusively a surface water bodies modelling system,

being the water column the core of the model structure. The sediment bed and the water surface where somehow static boundary conditions that were exclusively dependent of the water column processes. Thus, it was decided to perform a new reform in the code in order to enable a clear description of the contaminant transport model, and, most important, a clear description of environmental systems. The programming techniques used by MOHID revealed to be very important in this restructuring as they enabled a smooth and safe reorganization of the entire code.

In this chapter, a description is made on the programming approach (software engineering) followed in MOHID and on the final structure of the model, renamed to MOHID Water, with special emphasis paid to contaminant transport processes.

3.3. Software engineering

3.3.1. Object oriented programming paradigms

Scientific software developers often use FORTRAN as it is the most disseminated programming language among the scientific community. Its execution speed, versatility when operating with multidimensional arrays and complementary with mathematical libraries are some of the reasons of this popularity. FORTRAN 90 and 95 are revised versions of the language made in 1990's which enabled the usage of object-oriented programming (OOP) approach in an efficient way. OOP is a programming concept or approach that is being used, more and more, in software development. Some programming languages like JAVA, Visual Basic .NET, C++ or C# are known as object-oriented languages (OOL), which support "by default" the paradigms of OOP.

OOP bases its fundaments on objects, combining both data structure and behaviour of a single entity and generally includes aspects such as identity, classification, polymorphism and inheritance (Rumbaugh, 1991). Other recognized features are encapsulation and modularity. But, what is an object? Van Vliet (2000) distinguishes several viewpoints:

- the modelling viewpoint: an object is a entity, which distinguishes it from all other objects; objects have substance or properties;

- the philosophical viewpoint: objects are existential abstractions, as opposed to universal abstractions; entities that are created at some time, exist for some time and are ultimately destroyed;
- the software engineering viewpoint: objects are data abstractions, encapsulating data as well as operations on those data;
- the implementation viewpoint: an object is a contiguous structure in memory;
- the formal viewpoint: an object is a state machine with a finite set of states and finite set of functions;

Following the implementation viewpoint, objects can be achieved by instantiation of a class, i.e. the object is the "materialization" of the class (Leitão, 2003). A class is a piece of code designed to define the properties and operations of an object.

3.3.1.1. Encapsulation

An object contains a specific pack of memory which is kept encapsulated and can be shared with other objects through a Client/Server protocol. The server object defines which information can be accessed by the client by means of public properties and methods. Methods are operations or functions specific of an object that allow changing its state or properties. This hiding, broadly known as encapsulation, is a common feature of OOP, and by providing a fixed interface between objects, one achieves code modularity and flexibility, and one greatly simplifies the task of building a program in stages or programming in teams, since program components are naturally separated (Cary et al, 1997).

3.3.1.2. Inheritance

Inheritance, in the most general sense, can be defined as the ability to construct more complex (derived) classes from simpler (base) classes in a hierarchical fashion (Decyk et al, 1997a). It is understood as the sharing of structure and behaviour among classes in hierarchical relationship (Gray and Roberts, 1997), that is to say, a mechanism for deriving a new class from a base class. It provides a powerful code reuse mechanism since a hierarchy of related classes can be created and that share the same code (Akin, 2001). Inheritance is helpful in organizing modules that compose a particular application into a hierarchy that

indicates their relation to one another. A sensible hierarchy can be a great aid in managing the complexity of modern scientific computing application codes (Cary et al, 1997).

3.3.1.3. Polymorphism

Polymorphism can be defined as the behaviour of the same operation on different classes (Gray and Roberts, 1997). It allows different types of objects that share some common functionality to be used in code that requires only that common functionality. In other words, routines having the same generic name are interpreted differently depending on the class of the objects presented as arguments to the routines. This is useful in class hierarchies where a small number of meaningful function names can be used to manipulate different, but related object classes (Akin, 1999).

Another useful distinction is the difference between static (ad hoc) and run-time polymorphism. Static polymorphism means that the actual type being used at any point in the program is known at compile time, while run-time polymorphism means that a single type can refer to one of several possible actual types, and only at run-time can the correct type be determined (Decyk et al, 1998).

At the implementation level, polymorphism enables programmers to avoid writing inflexible, high-maintenance code in which objects must contain every possible behaviours and then use large IF-ELSE or switch code blocks to determine the desired behaviour at run time (Cary et al, 1997).

3.3.2. Object oriented programming using FORTRAN 95

FORTRAN 95 is the follow up standards of FORTRAN 90 programming language, with little differences, when compared to the upgrade from FORTRAN 77. FORTRAN 95 is not an object oriented language, but it goes a long way towards the goals of OOP. Bearing in mind the paradigms described above, these can, with some effort, be achieved using this "traditionally" non-object oriented language.

Modularity (MODULE statement) allows the programmer to perform encapsulation, by means of the PRIVATE statement. Still, encapsulation can become compromised in FORTRAN 95, as the language enables information to be changed outside an object, if a public method is created setting a POINTER to that information. This means that, although

a variable is defined to be PRIVATE inside a module, it can be changed if it is defined as a TARGET and a POINTER is pointed to it. If the POINTER is changed then the TARGET is also changed. To avoid this, one can duplicate information, allocating a new TARGET and equal it to the original TARGET, but duplicating code and memory, highly increasing execution and computational effort. This way, encapsulation in FORTRAN depends strongly on source code management and programming ruling.

Inheritance is achieved by means of the USE statement (see more in following paragraphs) and polymorphism using the INTERFACE statement, where a generic interface can be used to call a set of routines performing similar operations, defined with the MODULE PROCEDURE statement and differing on argument list. This is called function overloading in opposition to operators overloading, which stands for overloading built-in operators with new created operators to perform operations (e.g. with derived types) therefore becoming a very elegant coding feature. FORTRAN 95 does not include the full range of polymorphism abilities that one would like to have in an object-oriented language. Recently, FORTRAN 2003 standards were approved and many of these features will be included in the language.

3.3.3. Object oriented programming in MOHID

3.3.3.1. Overview

MOHID is designed in a modular way, each MODULE corresponding to class. The more than 50 classes that form MOHID were designed on a common basis, regarding programming rules and definition concepts in order to establish a straightforward connection of the whole code. This is reflected in memory organization, public methods systematisation, possible object states, client/server relations and errors management (Leitão, 2003).

Each class is responsible for managing a specific kind of information. The design of a class, in FORTRAN 95, can be accomplished by the MODULE statement. This way, information can be encapsulated using the PRIVATE statement. Encapsulation assures that all the information associated to an object is only changed by the object itself, reducing errors due to careless information handling in other classes.

```
module Class

    implicit none

    private
```

Figure 1 - Encapsulation in FORTRAN 95

The only two PUBLIC classes in MOHID are class *GlobalData* and class *Functions*: Class *GlobalData*, is responsible for global variables such as properties names and ID numbers, error types ID, constants and parameters, classes registration numbers and some derived types used frequently in other classes (e.g. type T_Size, a derived type containing the matrixes bounds); This is mainly static information needed and used equally by all classes. Some methods are also provided by this class, mainly related to checking properties names spelling and attributing ID numbers. It also handles error and used keywords logging and I/O units. Class *Functions* is a set of scientific mathematical functions or routines that are used by various others classes but that did not fit as specific methods of a class. This way this class can be seen as a run-time mathematical library included in the model.

3.3.3.2. A standard MOHID class

A standard MOHID class is defined as a derived type, which has, in addition to its specific information, two required structures: *InstanceID* and *Next*. *InstanceID* relates to the identification number of the class instance, that is the object's ID, which is attributed when the object is created.

```
private :: T_Class
type       T_Class
    integer                         :: InstanceID
    type(T_Class), pointer          :: Next
end type   T_Class
```

Figure 2 - Class standard structure in MOHID

Each time a new object is created, it is added to a collection of objects, stored in a linked list. *Next* relates to the object stored after the current in the list. The linked list is designed to be *one-way*, that is, it can only be scanned in one direction, because there was no need to turn it more complex (*two-way* or *four-way*) and it would only require more allocated memory.

Each class has only two global variables, defined as derived type pointers. They are the first object in the linked list (*FirstObject*), which works as an anchor or starting point to scan the list, and the current active object (*Me*).

```
type (T_Class), pointer         :: FirstObject
type (T_Class), pointer         :: Me
```

Figure 3 - Global variables in MOHID class

The procedure to access an object, is to, starting on the first object, scan the list and find the corresponding one through its ID number.

3.3.3.3. Object states and the object collector

A MOHID object can have two primary states: ON and OFF, standing for if the object has been constructed or not. In order to create a new object, the client object must use the constructor public method(s) which sets its state to ON. If a client object tries to access memory of another object that has not been constructed, therefore it does not exist, an error message is returned, which normally leads to stop execution. An object is only created once. In order to another client object access its information, the server object's ID must be provided by the constructor client so the instance is associated. This association is managed by the *Object Collector*. The *Object Collector* is a derived type array, placed in class *GlobalData*, where, in each array position, information is stored about the corresponding class instance. This information relates to the ID number of an object (*InstanceID*); the number of client objects associated to it (USERS) i.e. that can have access to it; the number of client objects reading information from it (READERS); and the object state (READ_LOCK).

```
type T_Instance
    integer                     :: ID         = 0
    integer                     :: Users      = 0
    integer                     :: Readers    = 0
    logical                     :: Read_Lock  = IDLE
end type T_Instance
```

Figure 4 - Object collector derived type structure

If an object is ON it can have two secondary states: READ_LOCK or IDLE. If an object is READ_LOCK it means that one or more client objects are accessing information, but without changing it. During this state, no public methods that lead to information alteration can be invoked. Each time a user stops reading, it invokes the READ_UNLOCK method, which removes one reader from the readers list. If no client objects are accessing information, then the object state is set to IDLE. This means although it exists, it is inactive. In order to read information from an object, the object must be IDLE or it must be READ_LOCK, as more than one reader is allowed.

In previous MOHID versions, an object could also have the WRITE_LOCK state (Miranda et al, 2000), but this feature was removed from the code as it was somehow redundant. The WRITE_LOCK state related to the phase when a client object modifies the object's information. This meant that others objects could not access or modify the information, as the object is in a transition phase. This state was first conceived to be used when performing parallel processing, as an object could not be read if it was still being modified, leading the program execution to wait and improving robustness in accessing memory. Although wise, this feature has proven to be unnecessary, once in all the code, never an object's public method is invoked when that object is WRITE_LOCK, because the locking and unlocking of this state was performed at the beginning and end of every public modifier method. This way, in order to be modified, an object must be IDLE, i.e. it must be ON but inactive, waiting for instructions.

Whenever invoking public methods and an inconsistency occurs in the client/server communication, a message is returned by the server indicating the type of error. Using this error message the client then decides the action to take: whether to continue without warning the user or send him a warning message and let him decide what to do, or stop execution if the error message compromises the program continuity.

3.3.3.4. MOHID objects methods

A MOHID class, following the OOP paradigm, has four types of methods: (i) Constructor – a new object creation or class instantiation; (ii) Selector - access to object information, performed as a read-only operation; (iii) Modifier - methods that modify the object state; (iv) Destructor - memory assigned to an object is freed.

In addition to these methods each class has management functions such as *Ready* which is called at the beginning of every public method and that checks the object state; and *LocateObject* which is the operation that locates an object in the objects linked list.

The constructor method consists in the following set of procedures:

- creating a new instance (client object calls constructor method);
- register the new instance in the object collector;
- checking for object state to be OFF avoiding the same object to be created twice;
- allocation of instance memory;
- addition of the object to module's linked list of objects;
- allocation and initialization of object properties;
- return instance ID to the client object;

Modifiers methods are used to modify the state variables of an object. When they are called, the correct instance of the module is located in the linked list through the instance ID, which is received from the client object by argument.

Selector methods are used to access encapsulated information of an object. All selector methods in MOHID start with the prefix "*Get*". Object location within the linked list is performed in the same way as in modifiers methods so that the selector method returns the desired information. For performance reasons, in the case of matrixes, the selector methods return pointer arrays. In this case, the state of the object providing the information is set to *READ_LOCK*, so it's protected against modification, once its information is accessed from outside of the object. The state turns to IDLE again, if the client module releases the pointer array by calling an "*UnGet"* method.

Destructor methods are used to remove an object from the modules linked objects lists. Like the Modifier and the Selector methods, the destructor methods receive the instance ID by argument from the client. After successfully locating the object, the memory used by the object is deallocated and the object is removed from the module linked objects list.

3.3.3.5. Input/Output as an OOP feature in MOHID

Class *EnterData* is the class responsible for input and output data to the model, and is used (inherited) by many other classes in MOHID. Objects created from this class open and read data files and store that information in memory, encapsulating it by means that the I/O unit is PRIVATE. They then provide client objects with public methods specific for accessing each type of information contained in the file. Polymorphism is applied when calling these methods as a generic interface *GetData* is used to extract information of varied types: integer, single or double precision, logical values, strings and arrays. When the data has been fully extracted, the object is destructed and the file closed. This application of OOP has proven to be quite useful as diminished input data errors and memory errors, as well as improved programming efficiency.

Input data for MOHID is based on ASCII files. This enables platform independency as the model is able to run without the use of a graphical user interface, normally designed specifically to each operating system (OS). The files are organized by keywords and information blocks, also defined by keywords, which can pile up to 3 hierarchical levels. This format can be seen likewise a simple Mark-up Language. File generation can be made manually or by using the graphical user interfaces (GUI). In order to use the same files both in MOHID and in the GUI, two classes were designed in FORTRAN 95 and in Visual Basic .NET (VB.NET), both sharing the same potentialities. This class (EnterData) has proven to be the triggering mechanism to the development team to enter the world of the developing stand-alone applications using the .NET platform. Developing GUI's using VB.NET, a fully OOL, is easy, fast and reliable when compared to the effort of designing them in Visual FORTRAN. This, on one hand, constrained the GUI development to a reduced number of programmers, resulting in task overloading, and on the other, inhibited the parallel evolution of the model and the GUI. With the "adoption" of VB.NET, this evolution is expected to be achieved, resulting in an important step towards reducing user input data errors.

User input data errors in MOHID can be estimated coarsely in near 90% of total execution errors, and can have two origins: user distraction or user unfamiliarity with the correct options (Leitão, 2003). Input data errors can be very time consuming, especially if the user wants quick answers. User distraction errors can be removed by using the GUI to generate

the data files and manage all the information. User unfamiliarity errors can be removed by the development of manuals and help files connected directly to the GUI. This is currently achieved using Compiled HTML Help files, which can be built using normal HTML files created in any common HTML editor and compiled using Microsoft HTML Help Workshop and connected to the VB.NET GUI, through a "Help Provider" object. Once the original files are written in HTML, their publication online is a straightforward task.

Output data files can have two formats: ASCII (time series) or HDF[1] (arrays). The time series files are also organized according to the input data files (keywords and information blocks). HDF format is OS and platform independent.

3.3.3.6. Parallel processing

Parallel processing has been recently been implemented in MOHID, by using MPICH[2], a free portable implementation of MPI, the standard for message-passing libraries. The historical need in numerical models to reduce computational time became a priority to the MOHID development team as an operational hydrodynamic and water quality model to the Tagus Estuary, in Lisbon, Portugal, was implemented using the MOHID Water model full capabilities (Braunschweig, 2004a, 2004b). The MOHID Water ability to run nested models was accomplished by creating a linked list of all the models and by attributing to each one a father-son identification, through which the models communicate. The first stage for introducing parallel processing in MOHID was to add the possibility of launching a process by each model to run, and then, using MPICH, establish communication between models. This enables each sub-model to run in a different processor (even if the processor belongs to a different computer, as long as it is in the same network) and in parallel, instead of running all in the same processor and each model having to wait for the others to perform their calculations. Parallel processing as it is presently implemented in MOHID, could not be achieved without object-oriented programming philosophy, as each model is an instance of class *Model* and no changes, exception made to the implementation of the MPI communications calls needed to be added. Using this feature, computational speed was improved (varying from application to application), as now the whole model will take the

[1] Hierarchical Data Format, developed at the National Center for Supercomputing Applications, http://www.ncsa.uiuc.edu
[2] http://www-unix.mcs.anl.gov/mpi/mpich

same time as the slowest model to run plus the time to communicate with the other processes. Here, the network communication speed plays an important role, as it can become limiting. Nevertheless, the amount of information passing between models, depending of course on the memory allocated for each model, has not yet proven to be time limiting.

3.3.3.7. Code Management

In a software project like MOHID, the number of programmers is both large and variable, turning source code management a primarily task. This effort must be made in order to maintain updated and reliable, the almost 250000 code lines that constitute the MOHID Water Modelling System.

MOHID source code management is accomplished by an internal set of rules, being the most important one, that any new code to be written in FORTRAN stands accordingly to the ANSI FORTRAN 95 standards. Besides that, all source code is kept under a data base project, provided by a specific software[3], which allows centralizing the source code files and keeping multiple versions of each file, as well as document all the changes performed. It performs graphical comparisons of different versions of each file and manages the user access to the code and prevents that more than one user changes the code in one file at the same time (Braunschweig, 2001). The possibility to access the historical record of the code has proven to be an important feature to improve the code robustness as it leads to a fast and reliable error detection.

3.4. Model structure

3.4.1. First approach

As referred before, MOHID was restructured in order to properly evolve as a sustainable water modelling system, which could include a contaminant transport model. The first step taken in this restructuring task was to study and revise the whole source code. MOHID "rotated" around four main modules, connected by the high level class module *Model*: class *Hydrodynamic* (computing hydrodynamic solution); class *WaterProperties* (eulerian

[3] Microsoft Visual Source Safe Explorer 6.0

transport model); class *Turbulence* (computing turbulent diffusion coefficients); and class *Lagrangian* (lagrangian transport model). To these four classes were provided boundary conditions in the bottom, by module *Bottom*, and at the water surface, by module *Surface*. Module *Bottom* computed shear, used to compute, not only the water flow, but also particulate matter transport processes and Module *Surface* provided wind velocities and/or stresses, solar radiation, air temperature, precipitation, evaporation, atmospheric pressure, etc. In order to couple the sediment compartment model to MOHID, it was defined that two new modules should be constructed. The strategy was to design a module, *SedimentProperties* (from a shell of module *WaterProperties*), able to compute sediment properties evolution, namely transport through porous media plus sinks and sources (which included as a first step, adsorption-desorption processes). This module should be able to exchange information with the water column model and also the surface model. In order to compute mass transport, water fluxes in the porous media had to be computed, so a new module was constructed: module *Consolidation*. The *SedimentProperties* module was connected directly to module *WaterProperties*, which proven to be an incorrect methodology, because fluxes at the water-sediment interface, which depended on the specific processes occurring there, such as shear stress, were not handled by the module that supposedly represented it, that is module *Bottom*. This lead to enormous effort in communication between modules as the hierarchical structure in which MOHID was designed, forced memory duplication and in difficult argument passing between modules.

3.4.2. Restructuring methodology

In order to convert, programmatically, environmental systems into a numerical model, an analysis of processes included in the model and the environmental compartments in which they take place, had to be conducted. Environmental systems can be divided into three compartments or media: air, water and land. This was the approach followed to restructure MOHID source code. As the code, derived from the fact that it was designed using an object oriented programming methodology, was already organized into modules (classes), each one handling a specific task, the reform was mainly performed at the high level of the model structure and in communications between modules (public methods), leaving the core of each class intact, in the generality of the modules.

Taking in advantage the fact that a reorganization of the code was to be performed, a global review was made, in order to clean it up from unused or obsolete features. An analysis of the existing modules was made, resulting in a classification into groups of modules that had common tasks or purposes. This resulted into six functional groups of modules:

Global parameters modules – modules which handle global parameters like recognized property lists, time handling and functions, etc (e.g. *GlobalData*, *Time*);

Independent functions modules – modules that handle specific operations (e.g. *Functions* – various mathematical or scientific functions, *Triangulation* – performs advanced triangulation, *LUD* – equations systems solver);

Structural modules - modules that handle geometry domain discretization and referentials, using variables like distances, areas, volumes, compute points, etc. (e.g. *HorizontalGrid* – handles the horizontal discretization, *HorizontalMap* – handles 2D horizontal mapping of grid cells like covered and uncovered cells, *Map* – handles 3D mapping of grid cells, *Geometry* - handles the vertical discretization and volumes);

Data handling modules – modules that perform I/O operations (e.g. *EnterData* – reads and writes ASCII data files, *HDF5* – reads and writes matricial data into HDF5 format, *TimeSerie* – reads and writes formatted time series ASCII files);

Specific functions modules – modules that perform specific operations that can only be used in MOHID (e.g. *BoxDif* - divides 2D and 3D domains into boxes and computes exchanges between boxes, total mass inside a box or process rates within a box, *Statistics* - computes basic statistic operations over space and time, *Interface* - interface between 3D and 0D models, *WaterQuality* – eutrophication module);

Processes modules - modules that correspond to the different processes taking place in the different environmental compartments (Hydrodynamic, WaterProperties, Turbulence, Lagrangian, Bottom, Surface);

This approach was useful as it served as a global review of the hierarchic tree that constituted the model.

As the main problems in connecting the sediment module into MOHID were identified in the communication with the water column modules (*Hydrodynamic* and *WaterProperties*)

through module *Bottom*, it became clear that the three environmental compartments should be able to communicate in an easy and straightforward way. This lead to a following design: one model consisting of two main interfaces: the water-sediment interface and the water-air interface, dividing three well defined compartments, the atmosphere, the water column and the sediment. The two interfaces should be able to communicate by handling the fluxes between the three compartments. To do this, two modules were created: module *InterfaceSedimentWater* and module *InterfaceWaterAir*. The first was designed based on module *Bottom* and the second based on module *Surface*, which was split into two modules: module *InterfaceWaterAir* and module *Atmosphere*. The interface module was now responsible by processes occurring at the water-air interface, such as computing wind shear stress, radiation balances, latent and sensible heat fluxes; and the atmospheric module by processes occurring in the atmosphere like wind velocity, radiation, cloud cover or precipitation (although not explicitly calculated, rather serving as a database of meteorological and atmospheric modules).

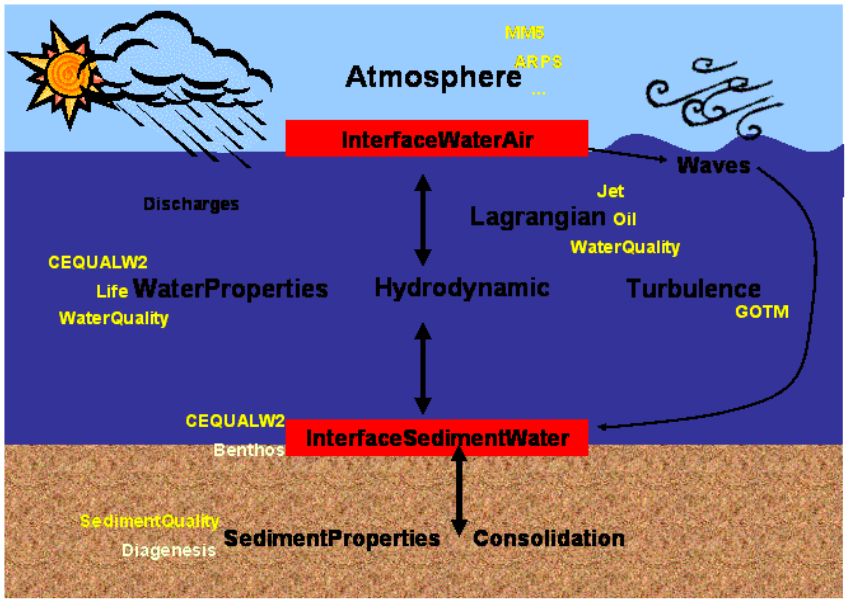

Figure 5 - MOHID modular structure

Thus, the model was set up in a way that each of the three compartments did not have access to another compartment, being all communications made by the interface modules. That is, with this organization, modules *SedimentProperties* and *Consolidation*

(representative of the sediment column), communicate only with the *InterfaceSedimentWater* module, as well as modules *Hydrodynamic*, *WaterProperties*, *Turbulence* and *Lagrangian* (representative of the water column). These modules also communicate with module InterfaceWaterAir which provides the connection with module *Atmosphere*. Module *Model* controls and manages all the information fluxes.

3.5. Contaminant transport model

3.5.1. Modelling approaches

A model must be adjusted to the system and to the processes it pretends to simulate. Transport models have normally two different approaches: eulerian and lagrangian.

Eulerian methods compute the evolution of a property in a fixed collection of points in space. These models solve the advection-diffusion equation and need velocity fields and diffusion coefficients, being normally coupled with hydrodynamic models. They are limited by stability and precision of the numerical methods used (spatial and temporal discretization) and by representation of the sub-grid mixing in the diffusion term. The diffusion term represents molecular dynamics or the unresolved advection terms. The overwhelming majority of numerical transport models use spatial and time discretization larger than the processes associated with the properties of the flow; therefore for estuarine and coastal waters turbulent flows, the effective diffusivity is several orders of magnitude greater than the molecular diffusion, having to be parameterized. The modeller must always have in mind these limitations, namely in contaminant transport studies, where maximum concentrations can be desired as a result, rather than medium grid cell concentrations.

Lagrangian models, also known as particle tracking models, are normally based on tracers, in which properties evolution is followed in the tracer referential rather then in a fixed referential. These models are useful as they explicitly solve the advection term avoiding instability problems, being precision only dependent of the number of tracers and indirectly of the precision with which the hydrodynamic model computes the flow field and of the local turbulence characteristic parameters (Leitão, 1996). This methodology is normally used to simulate systems with steep gradients (e.g. river plumes, pollutant discharges).

3.5.2. Conceptual model

In order to simulate contaminant transport processes, the concept of particulate and dissolved phases had to be created in properties simulated by MOHID Water. This concept already existed in MOHID but it was implicitly applied only to cohesive sediments. In order to simulate a variety of contaminants, this notion was stated and it was applied both in the water column and the sediment column.

3.5.2.1. Water column

The water column entity is embodied by module *WaterProperties* which uses module *Hydrodynamic* to compute water fluxes that are then used to compute water properties transport. MOHID Water is prepared to simulate properties such temperature, salinity, cohesive sediments, phytoplankton, nutrients, contaminants, etc. These properties can either be dissolved in the water, therefore following the currents, or in a particulate phase or adsorbed on to particulate matter, thus being subjected to one more transport variable: the settling velocity. This enables particulate properties to deposit in the bottom and thus become a part of the sediments.

3.5.2.2. Sediment column

Module *SedimentProperties* is responsible by handling the sediment compartment. The sediment column consists of a saturated porous media, formed by sediments and by water that fills the interstices between the sediments. Properties in this compartment can also be dissolved - in the porewater-, or particulate – adsorbed on to sediments.

3.5.2.3. The sediment-water interface

The sediment-water interface handles processes occurring between the water and the sediment column. This interface is an abstraction, as physically it is very difficult to define. In the model, it can be seen as a thin sediment layer (fluff-layer) with transient characteristics, depending basically on temporal scales associated with hydrodynamics and transport in the water column, namely erosion and deposition. This layer has a separation function, which allows dissociating processes that occur on the sediment deposit, at a very slow scale, “filtering” the high frequencies of erosion/deposition fluxes that shape it, therefore leading to consolidation.

Dissolved properties can be produced in the interface but their mass is not part of it, becoming part of the water column by means of a boundary condition flux. On the contrary, particulate properties are acquainted in the sediment-water interface. This can be the case, when sediment deposition occurs but the sediment is not yet consolidated. Thus, a particulate property deposited mass is tracked in order to know how much of is available when erosion conditions occur. Following this concept, it is considered that dissolved properties can exchange fluxes directly between the water column and the sediment interstitial water. In erosion conditions, if this transient layer is completely eroded, then scouring is made from the sediment compartment upper layer, where consolidated sediment is present. When this happens, interstitial water is dragged along with the sediment, therefore constituting a flux to the water column. The same way, when the fluff-layer consolidates and becomes part of the sediment column, there is an input of overlaying water (and its properties) to the sediment compartment.

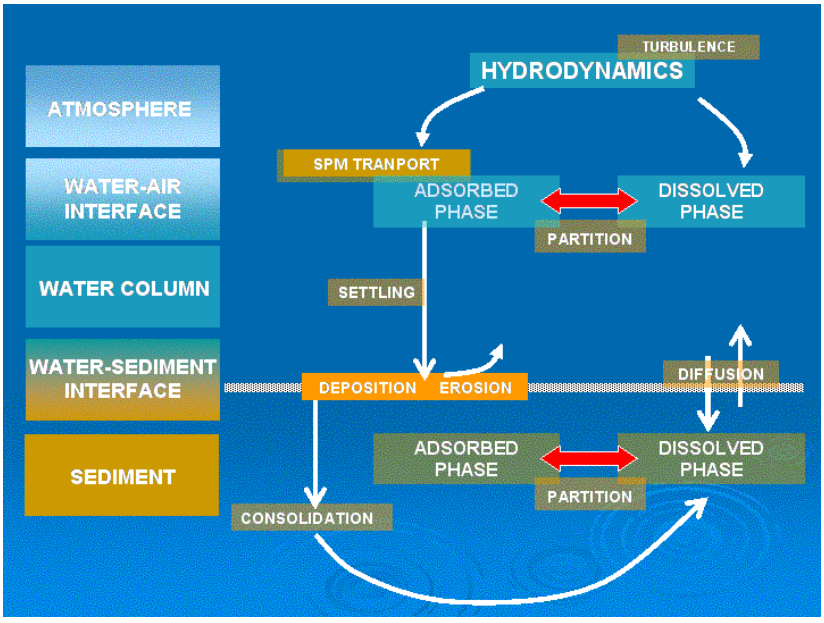

Figure 6 - MOHID contaminant transport model processes

3.5.3. Boundary conditions

The interpretation of transport phenomena through a numerical model requires that appropriate boundary conditions are provided. These boundary conditions can be provided at the surface and bottom of the domain and on the lateral boundaries, and can be closed, open or mobile. Imposed values, inwards-outwards fluxes, decaying laws can be imposed depending in the type of boundary. Mobile boundaries are closed boundaries whose position

varies in time, e.g. covered/uncovered zones such as tidal flats, due to the tidal water level variations. This type of boundaries is mainly applied in the water column modules, but, nevertheless influences the sediment compartment as its surface boundary is modified.

Still in the water column, any flux between land and water, such as a river or an effluent, is computed as a discharge. Discharges can contain hydrodynamic properties (e.g. momentum), or water properties (e.g. temperature, salinity, suspended particulate matter, pollutant loading).

The open boundary can correspond, for example, to the oceanic boundary. In estuarine model applications tide is imposed at the open boundary, where water level is normally imposed after being computed through tidal harmonic components. Open boundary conditions is a "science" within hydrodynamic and transport modelling. An extensive overview on how this type of boundaries is handled in MOHID Water can be found in Leitão (2003).

3.5.4. Water column model

3.5.4.1. Hydrodynamics

The hydrodynamic class solves the primitive continuity and momentum equations for the surface elevation and 3D velocity field for incompressible flows, in orthogonal horizontal coordinates and generic vertical coordinates, assuming hydrostatic equilibrium and Boussinesq approximation. The mass and momentum evolution equations are:

$$\frac{\partial u_i}{\partial x_i} = 0$$

$$\frac{\partial u_1}{\partial t} + \frac{\partial \left(u_j u_1\right)}{\partial x_j} = -fu_2 - g\frac{\rho_\eta}{\rho_0}\frac{\partial \eta}{\partial x_1} - \frac{1}{\rho_0}\frac{\partial p_S}{\partial x_1} - \frac{g}{\rho_0}\int_z^\eta \frac{\partial \rho'}{\partial x_1} dx_3 + \frac{\partial}{\partial x_j}\left(A_j \frac{\partial u_1}{\partial x_j}\right)$$

$$\frac{\partial u_2}{\partial t} + \frac{\partial \left(u_j u_2\right)}{\partial x_j} = fu_1 - g\frac{\rho_\eta}{\rho_0}\frac{\partial \eta}{\partial x_2} - \frac{1}{\rho_0}\frac{\partial p_S}{\partial x_2} - \frac{g}{\rho_0}\int_z^\eta \frac{\partial \rho'}{\partial x_2} dx_3 + \frac{\partial}{\partial x_j}\left(A_j \frac{\partial u_2}{\partial x_j}\right)$$

$$\frac{\partial p}{\partial x_3} = -\rho g$$

Where u_i are the velocity vector components in the Cartesian x_i directions, η is the free surface elevation, f the Coriolis parameter, A_i the turbulent viscosity and p_s is the atmospheric pressure. ρ is the density and ρ' its anomaly.

Density is computed depending on salt, temperature and pressure, by the UNESCO equation of state (UNESCO, 1981).

The model uses an ADI (Alternate Direction Implicit) time discretization scheme which minimizes stability restrictions, and is defined in an Arakawa-C type grid. Turbulence is computed through a set of available models:

Horizontal turbulence - Constant, Smagorinsky (1963), Proportional to depth and to the square of velocity;

Vertical turbulence – Constant, Nihoul (1984), Leendertse and Liu (1978), Backhaus and Hainbucher (1987), Pacanowski and Philander (1981), and GOTM (Burchard et al, 1999) – http://www.gotm.net, a turbulence models library coupled with MOHID, including a k-ε model and Mellor-Yamada second order turbulent closure model (Mellor and Yamada, 1982).

In the bottom, shear stress can be computed with the assumption of a logarithmic velocity gradient:

$$\tau = \rho C_d \left|\vec{u}_+\right| \cdot \vec{u}_+ \qquad C_d = \left[\frac{k}{\ln\left(\frac{z_+ + z_0}{z_0}\right)} \right]^2$$

Where τ is the bottom shear stress, u_+ is the velocity field at a distance z_+ above the bottom, C_d is the roughness coefficient, k is the Von Karman constant and z_0 is the bottom roughness length.

In the free surface, momentum flux can also be imposed in the form of shear stress.

Momentum, mass and heat transport is computed using a generic 3D advection-diffusion library including various advection schemes namely: first, second and third order upwind, centred differences and TVD (Total Variation Diminishing). Advection is solved in the three directions as a one-dimensional case and various time discretizations can be combined: explicit, semi-implicit or fully implicit.

3.5.4.2. Dissolved properties eulerian transport in the water column

Transport phenomena in the water column for a given property (P), can be described by the 3D advection-diffusion differential equation:

$$\frac{dP}{dt} = \frac{\partial P}{\partial t} + u_j \frac{\partial P}{\partial x_j} = \frac{\partial}{\partial x_j}\left(k_\Theta \frac{\partial P}{xj}\right) + (Sources - Sinks)$$

P is the concentration (ML^{-3}), j is the index for the correspondent Cartesian axis (x_1, x_2, x_3) or (x,y,z), K_Θ is the turbulent mass diffusion coefficient (horizontal/vertical). Sources and sinks related to reaction processes taken place inside the assumed control volume, which undertakes local production and destruction terms.

3.5.4.3. Particulate properties eulerian transport in the water column

Particulate properties transport is governed by a 3D advection-diffusion equation where the vertical advection includes the particle settling velocity.

$$u_Z = u_{Z'} + w_S$$

Where u_z is the overall vertical velocity of the particulate property, $u_{z'}$ is the vertical current velocity, and w_s is the property's settling velocity. This methodology enables to compute particulate properties transport, like particulate contaminants or particulate organic matter, likewise and dependent of cohesive sediments.

Two different approaches are followed to compute settling: a constant settling velocity and a cohesive sediment concentration dependent settling velocity. In the first case, each particulate can have its specific and constant settling velocity, which can be derived from literature (depending on its size and biogeochemical characteristics). The latter approach, however, needs some considerations. As the settling velocity algorithm was developed for cohesive sediment modelling, how can the other particulate properties settling velocity be computed? In this study, it is considered that it is the same as the cohesive sediment settling velocity, therefore reinforcing the importance of cohesive sediments in the distribution and fate of the adsorbed contaminants fraction. The algorithm follows formulation widely used in literature (e.g. Mehta, 1988), where the general correlations for the settling velocity in the flocculation range are:

$$W_S = K_1 C^m \qquad \text{for} \quad C < C_{HS},$$

and in the hindered settling range is:

$$W_S = K_1 C_{HS}{}^m \left[1.0 - K_2 \left(C - C_{HS}\right)\right]^{m_1} \qquad \text{for} \quad C > C_{HS}$$

where Ws (ms^{-1}) is the settling velocity, C (kgm^{-3}) is the concentration, and the subscript HS refers to the onset of the hindered settling (of about 2 to 5 kgm^{-3}). The coefficients K_1 ($m^4kg^{-1}s^{-1}$) and K_2 (m^3kg^{-1}) depend on the mineralogy of the mud and the exponents m and m_1 depend on particle size and shape.

3.5.4.4. Adsorption/Desorption

Adsorption and desorption are considered as a reaction process, that can be included in the sinks and sources terms of contaminants transport equation. This reaction involves the dissolved and the particulate phases of the contaminant being simulated, where the two phases tend to an equilibrium, which is given by a partition coefficient. The equilibrium can be described by the following system of equations (Hayter and Pakala, 1989)

$$\frac{\partial C_d}{\partial t} = k\left(\left(D\% \times C_p - P\% \times C_d\right)\right.$$

$$\frac{\partial Cp}{\partial t} = k\left(\left(P\% \times C_d - D\% \times C_p\right)\right.$$

C_p and C_d are the particulate and dissolved contaminant concentrations respectively; k (s^{-1}) is the equilibrium kinetic rate for adsorption-desorption between dissolved and particulate phase; D% is the dissolved contaminant fraction; and P% the particulate contaminant fraction.

The kinetic constant defines the rate at which the two phases tend to equilibrium. To account for the fact that, in the presence of low suspended matter concentrations, the adsorption process is less probable to occur (the probability of a contaminant ion to hit a particle is lower), a direct relation between the kinetic rate and the suspended particulate matter was implemented, where:

$$\begin{cases} k = k_{ref} \cdot \dfrac{C_{SPM}}{C_{SPM\ reference}} & for \quad \dfrac{C_{SPM}}{C_{SPM\ reference}} < 1 \\ k = k_{ref} & for \quad \dfrac{C_{SPM}}{C_{SPM\ reference}} \geq 1 \end{cases}$$

3.5.4.5. Lagrangian tracers

As described above, contaminants in the water column can be simulated through lagrangian tracers approach (Leitão, 1996).

$$\frac{dx_i}{dt} = u_i(x_i, t)$$

where u stands for the mean velocity and x for the particle position. Velocity at any point of space is calculated using a linear interpolation between the points of the hydrodynamic model grid. Turbulent transport is responsible for dispersion. The effect of eddies over particles depends on the ratio between eddies and particle size. Eddies bigger than the particles make them move at random. Eddies smaller than the particles cause entrainment of matter into the particle, increasing its volume and its mass according to the environment concentration. The random movement is calculated following the procedure of Allen (1982). The random displacement is calculated using the mixing length and the standard deviation of the turbulent velocity component, as given by the turbulence closure of the hydrodynamic model. Particles retain that velocity during the necessary time to perform the random movement, which is dependent on the local turbulent mixing length (Leitão, 1996).

Settling velocity of a tracer can be computed based on its diameter, therefore enabling the modelling a range of particle sizes, with different settling velocities.

3.5.5. Water-sediment interface model

The water sediment interface model computes and manages boundary conditions for the water column and sediment compartments.

3.5.5.1. Cohesive sediments fluxes

For cohesive sediments at the bottom, a flux term, F_b, (mass of sediment per unit bed area per unit time) can be defined, corresponding to a source or sink for the suspended particulate matter in conditions of erosion or deposition, respectively. Consequently, at the bottom:

$F_b = F_E - F_D$

where F_E and F_D are respectively the erosion and deposition fluxes.

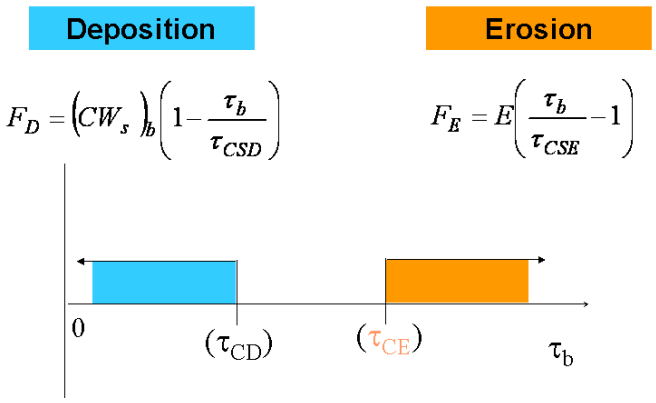

Figure 7 – Erosion and deposition modelling algorithm

It is assumed that, when bottom shear stress is smaller than a critical value for deposition, there is addition of matter to the bottom, and, when the bottom shear is higher than a critical value, erosion occurs. Between those values, erosion and deposition balance each other. The erosion algorithm used is based on the classical approach of Partheniades, (1965). Erosion occurs when the bottom shear stress exceeds the threshold of erosion. The flux of eroded matter is given by:

$$\begin{cases} F_E = E\left(\frac{\tau}{\tau_E}-1\right) & for \quad \tau_b > \tau_{CSE} \\ F_E = 0 & for \quad \tau_b < \tau_{CSE} \end{cases}$$

where τ is the bed shear stress, τ_{CSE} is a critical shear stress for erosion and E is the erosion parameter ($kgm^{-2}s^{-1}$). This erosion algorithm is computed at the sediment-water interface (fluff-layer). If this layer is eroded, erosion occurs from the underlying sediment layer, which has a higher level of compaction, therefore increasing the erosion shear stress thresholds. This is obtained by defining τ_{CSE} as depth dependent, reflecting the increasing resistance of the sediment to be eroded as scouring reaches deeper layers. Wave induced shear stress can also be computed by the model by a linear wave theory, given wave characteristics such as wave period and wave significant height. Estuarine local waves can be important in terms of sediment resuspension, especially in shallow water where the wave stresses effect reaches the sediment bed. Pina (2001), presents a detailed description on the formulation implemented in the model.

On the other hand, the deposition flux can be defined as:

$$F_D = -p(W_S C)_b$$

where p is the probability of sediment particles to set down on the bed; W_S is near-bed the settling velocity; and C the near-bed cohesive sediment concentration. The probability of deposition (Krone, 1962), can be defined as:

$$p = (1 - \frac{\tau_b}{\tau_{CSD}})$$

where τ_b (Pa) and τ_{CSD} (Pa) are the bottom shear stress and the critical shear stress for deposition respectively. This concept reflects the fact that the deposition of flocks is controlled by near-bed turbulence. For a flock to stick to the bed, gravitational forces must be strong enough to withstand the near bed shear stress. The deposition algorithm (Krone, 1962), like the erosion algorithm, is based on the assumption that deposition and erosion never occur simultaneously, i.e. a particle reaching the bottom has a probability of remaining there that varies between 0 and 1 as the bottom shear stress varies between its upper limit for deposition and zero respectively. Deposition is calculated as the product of the settling flux and the probability of a particle to remain on the bed:

$$\begin{cases} F_D = (CW_S)_B(1 - \frac{\tau}{\tau_{CSD}}) & for \quad \tau_b < \tau_{CSD} \\ F_D = 0 & for \quad \tau_b > \tau_{CSD} \end{cases}$$

The critical shear stress for deposition depends mainly on the size of the flocks. Bigger flocks have higher probability of remaining on the bed than smaller flocks. As a single characteristic class of cohesive sediment is considered in the model, parameters must subject to calibration, starting from reference values found in literature, in order to achieve good approximations in the final results.

Consolidation, in this study, was considered to occur on recently deposited sediments at the sediment-water interface, and was modelled as a sediment flux, $F_{consolidation}$ ($kg_{sed}m^{-2}s^{-1}$), between the fluff layer and the first sediment layer at a certain rate, $k_{consolidation}$ (s^{-1}), dependent on the sediment mass per unit of area deposited at the fluff layer. It is assumed that consolidation only occurs when shear stress (τ_b) is lower than the critical shear stress for deposition (τ_{CSD}).

$$\begin{cases} F_{consolidation} = 0 & for \quad \tau_b > \tau_{CSD} \\ F_{consolidation} = M_{sediment} \cdot k_{consolidation} & for \quad \tau_b < \tau_{CSD} \end{cases}$$

This consolidation flux is one of the governing processes for particulate contaminant fractions to enter the sediment compartment.

3.5.5.2. Particulate properties fluxes

Particulate properties fluxes at the sediment-water interface depend on erosion and on consolidation processes.

As the erosion algorithm was developed specifically for cohesive sediment modelling, when computing other particulate properties fluxes at the bed, the erosion rate parameter cannot be the same. Thus, a specific proportionality factor for the erosion constant is computed, E_{prop}, for each property, relating the quantity of property ($M_{property}$ – $kg_{property}m^{-2}$) to the quantity of cohesive sediment deposited in the bed ($M_{sediment}$ – $kg_{sed}.m^{-2}$). The particulate property erosion flux is then computed similarly to cohesive sediments but with a specific E_{prop}.

$$E_{prop} = E\left(\frac{M_{property}}{M_{sediment}}\right)$$

This way, critical shear stress values are considered equal for all particulate properties, being the specific erosion constant the differentiating factor.

When consolidation occurs, a similar algorithm is followed, relating the sediment consolidation flux with the particulate property deposited mass. Thus, the property consolidation flux (F^{prop}) can be computed as in the following expression:

$$F_{consolidation}^{prop} = F_{consolidation}^{sediment}\left(\frac{M_{property}}{M_{sediment}}\right)$$

3.5.5.3. Dissolved properties

Dissolved properties fluxes across the water-sediment interface depend both on erosion/consolidation processes and on concentration gradients between the water column's lower layer and on the interstitial water of the sediment's upper layer.

As stated before, when the fluff-layer is active (i.e. there are recently deposited sediments on the bed), interstitial water between those sediment particles is not considered. Thus,

when erosion occurs, there is no dissolved properties income from the fluff layer to the water column.

In the sediments' upper layers, interstitial water (containing solutes such as dissolved contaminant fractions, nutrients, etc) is flushed to the water column when consolidated sediment is eroded (upper sediment compartment layer). On the other hand, when consolidation occurs, water overlying the sediment bed becomes part of sediment's interstitial water. These processes constitute an additional flux of solutes to and from the water and sediment columns. Thus, a water flux (F^{water} – m^3s^{-1}) can be computed, corresponding to the amount of porewater dragged along with the eroded sediments or to the amount of overlying water dragged in the consolidation process:

$$F^{water}_{erosion/consolidation} = F_{Erosion/consolidation} \cdot A \cdot \phi_k \cdot \frac{1}{\rho_{sed} \cdot (1-\phi_{kn})}$$

Where, $F_{erosion/consolidation}$ is the cohesive sediment flux ($kg_{sed}m^{-2}s^{-1}$) between the sediment-water interface and the sediments' upper layer, Φ_{kn} is the porosity in the upper (k=n) sediment layer, ρ_{sed} is the sediment dry density ($kg_{sed}m_{sed}^{-3}$) and A is the area (m^2) of the sediment-water interface. Respectively, solute fluxes are given by:

$$F^{solute}_{erosion/consolidation} = \frac{F^{water}_{erosion/consolidation} \cdot C^{solute}}{A}$$

where C is the solutes' concentration ($kg.m_{water}^{-3}$) in the sediment upper layer or in the water column bottom layer, depending on the type of flux (erosion or consolidation).

As mentioned above, the concentration gradients between the water column bottom layer and the sediment surface layer can also produce a mass flux through the sediment-water interface. Solutes, in a turbulent flow can be transported by a mean advective flux, turbulent diffusion and molecular diffusion. It is usually considered that solutes diffusion coefficient is equal to the fluids' turbulent viscosity, which is normally several orders of magnitude higher. Nonetheless, when approaching the sediment bed, water flow is reduced, as well as turbulent movements, leading to the increase of molecular diffusion importance in relation with the turbulent one. Thus, a sub-diffusive layer (Boudreau, 1997) is formed, where a linear concentration gradient can be considered, and a diffusive flux, $F_{diffusive}$ ($kg_{solute}m^{-2}s^{-1}$), can be computed representing the rate at which this gradient tends to be eliminated:

$$F_{diffusive} = \frac{D_{molecular}}{\delta} \cdot A \cdot (C_{water} - C_{interstitial})$$

In which $D_{molecular}$ is the molecular diffusion coefficient (m^2s^{-1}), and δ (m) is the sub-diffusive boundary layer thickness, which is dependent on near-bed turbulence:

$$\delta = \frac{2 \cdot \nu_{water}}{u_+}$$

Where υ_{water} is the water cinematic viscosity (m^2/s) and u_+ is near-bed shear velocity (m/s).

3.5.6. Sediment column model

The sediment column model is basically a set of 1D vertical models defined below the 3D water column model. Both models share the same horizontal discretization, but compute independent vertical coordinates. As referred above, the sediment column model was in practice based on the water column strategy, and constitutes the core of the advances made in the framework of this study.

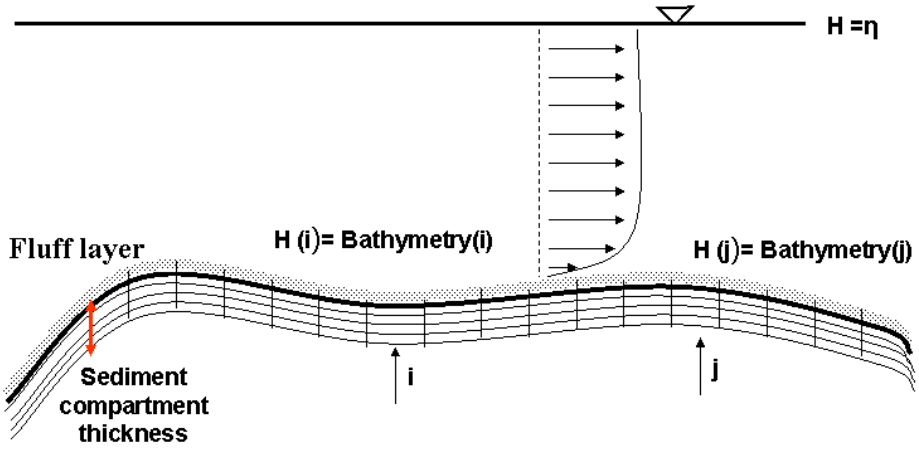

Figure 8 – Sediment compartment discretization

3.5.6.1. Sediment physical processes and properties

The sediment compartment is constituted by a module which computes the sediment geometry (variations due to erosion and consolidation), namely dry sediment volumes and

interstitial water volumes. In terms of vertical referential, it is located below the water column until a certain defined depth. The construction of the domain is made by means of a depths file, similar to the bathymetry for the water column model. This way, sediments' upper layer is located at the same coordinate of the water column model bathymetric value, with a certain depth, usually 10 to 30 cm (Figure 8).

This compartment is considered to be a saturated porous media, so a key variable is porosity (Φ), which represents the fraction of volume occupied by interstitial water. Porosity decreases with depth and relates to tortuosity, a parameter which reflects the influence of porous media geometry in the transport phenomena, namely diffusion. Tortuosity can be seen as an extension of the path a solute has to take in the porewater, due to the fact that, it has to follow a complex structure of micro-channels in the available spaces between sediment particles. Boudreau (1996), finds a good agreement between tortuosity and porosity:

$$T_f = 1 - \ln(\phi^2)$$

A decay of porosity can be computed, accounting for the consolidation process.

$$\frac{\partial \phi}{\partial t} = \frac{\phi_\infty - \phi}{\lambda}$$

Where Φ_∞ is the porosity of a fully consolidation sediment and λ is decay factor (s). This consolidation process has a time scale several times higher than the erosion/deposition processes and in this study is neglected. However, it is included in the model, and can be useful in long term simulations, has when consolidating, interstitial water is pushed upwards, therefore advecting solutes through the sediment column, and even through the water-sediment interface onto the overlying water column. These fluxes can also be accounted as a source of contaminants to the water column.

The sediment compartment boundary conditions were described above, and consist on the erosion and consolidation fluxes, and are controlled by the sediment-water interface module. Erosion is made, by removing material from the sediments' upper layer. As sediment layers are being scoured, critical shear stress increases, due to the fact that sediments compaction level increases with depth. Therefore, critical shear stress can be computed such as:

$$\tau_{CSE(z)} = \tau_{CSE(z=\infty)} + (\tau_{CSE(z=0)} - \tau_{CSE(z=\infty)})e^{-\frac{z}{\psi}}$$

Where z is the depth (m) and Ψ is a decay coefficient (m).

A specific new algorithm was developed to solve discretization problems of a complex vertical domain, like the sediment compartment. The vertical resolution must be high enough to solve properly the sharp concentration gradients (contaminants, organic matter, oxygen, etc) existing in estuarine sediments. Two main problems can be found: the sediment top layer is constantly eroded until it disappears; or the deposition flux is so high that the top layer thickness increases to a level that it cannot be assumed that properties inside the layer are constant. Thus, in order to handle these problems two thickness limitations were imposed: a minimum and a maximum layer thickness.

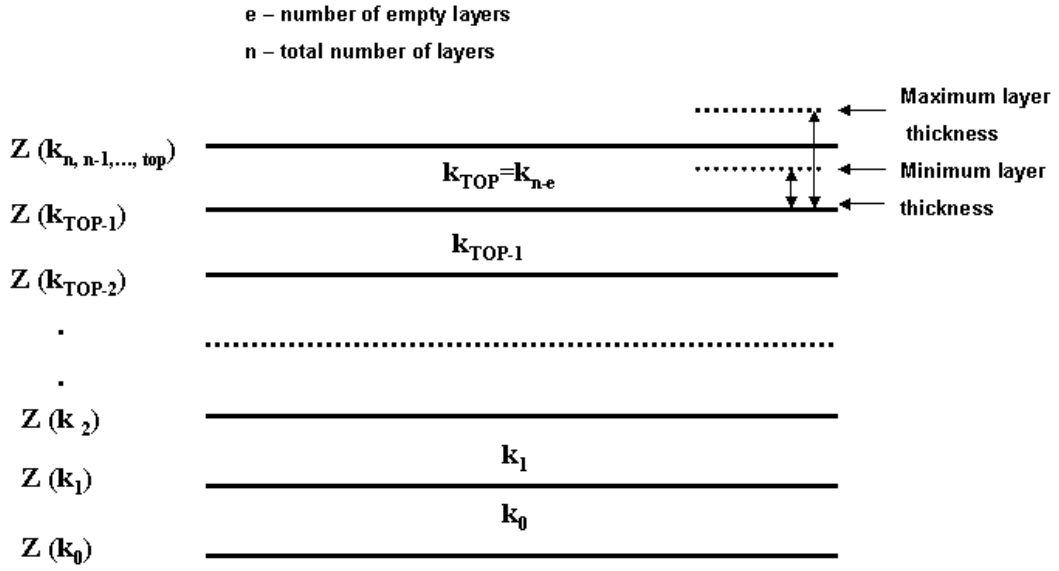

Figure 9 – Representation of the vertical discretization of a 1D sediment column.

When erosion fluxes remove material from the sediments' compartment upper layer, this flux is limited so that, in one iteration, the layer does not exceed the minimum layer thickness. When this happens, the upper layer collapses and becomes part of the lower layer, which then, becomes the top layer.

When consolidation fluxes raise the top layer thickness so that it exceeds the maximum layer thickness, a new layer is created, splitting the upper layer into two. The new upper layer is initialized has having the minimum layer thickness allowed.

To overcome these problems, a new vertical coordinate system was created to account for collapsing and splitting of layers. A two-dimensional mapping variable monitors which is the index of the top layer, above which, all water and sediment volumes are null, as well as all processes. The model must always be started with a certain number of empty top layers to account for possible creation of new layers, if consolidation occurs. If the initial number of layers is exceed, the model stops. The same happens when all sediment layers are eroded and collapsed.

The layers collapsing and splitting is followed by mass conserving algorithms applied to each of the sediment properties, both dissolved and particulate.

3.5.6.2. Dissolved properties

Transport of dissolved properties in porewater is computed only in the vertical axis, as horizontal gradients are not considered in this study. Therefore, the transport equation can be written:

$$\frac{\partial(C_d)}{\partial t} + \frac{\partial((w)C_d)}{\partial z} = \frac{\partial}{\partial z}(k_z \frac{\partial C_d}{\partial z}) + (Sources - Sinks)$$

Where C_d is the concentration ($kg.m_{water}^{-3}$), w (m/s) is the porewater velocity due to compaction, k_z (m^2s^{-1}) is the diffusivity coefficient. The molecular diffusion coefficients must be corrected with tortuosity parameterization, to account for the increase in the solute pathways due to difficulty presented by the sediment particles for diffusion to occur. Two different formulations (Figure 10) were included in model, the first following formulation by Berner (1980), tortuosity dependent, which on the other hand is porosity dependent:

$$D_m = D_{INF} \cdot \frac{1}{T_f^{\,2}}$$

The second by Soetaert (1996), is dependent of porosity square.

$$D_m = D_{INF} \cdot \phi^2$$

Where, D_{INF} (m^2s^{-1}) is the molecular diffusion coefficient in solution, and D_m (m^2s^{-1}) is the corrected molecular diffusion coefficient.

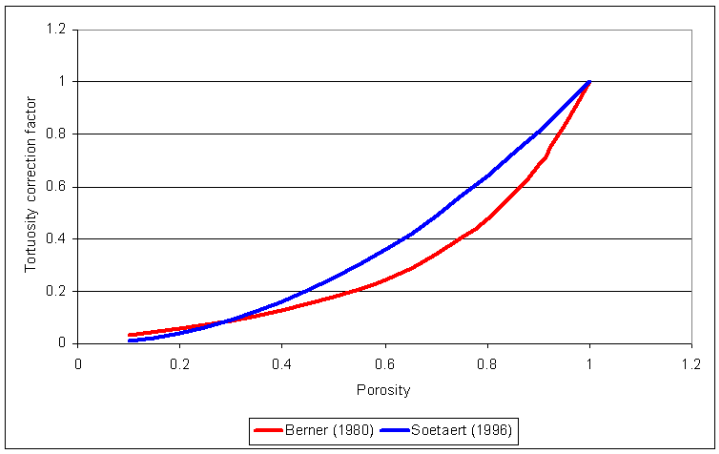

Figure 10 – Comparison between the two formulations used to compute tortuosity correction factor

Bioturbation is computed as a diffusion coefficient, which is present until a certain depth, and decreases exponentially with it. This pretends to simulate benthic fauna activity, which is most of the times present in sediments upper 10-15cm. Below this, bio-activity can be considered negligible. Thus, the bioturbation diffusion coefficient, D_b (m^2s^{-1}), can be computed by:

$$D_b = \begin{cases} D_b & for\ z < z_b \\ D_b \cdot e^{\left(\frac{-z-z_b}{\alpha}\right)} & for\ z > z_b \end{cases}$$

In which z_b is the depth limit for maximum biological activity and α is a decay coefficient (m) to account for the decrease of bioturbation with depth.

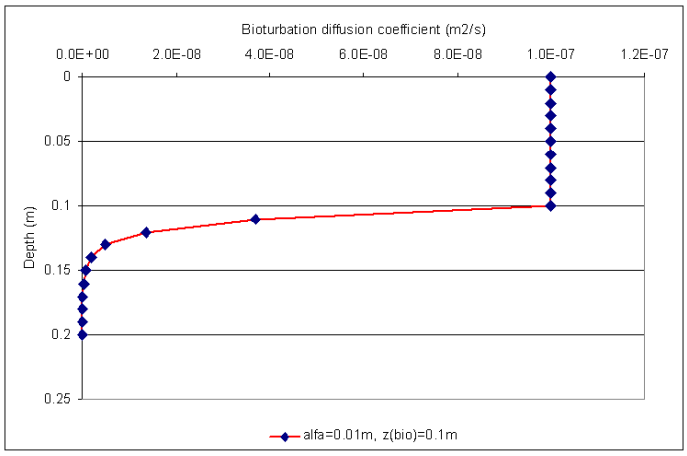

Figure 11 - Bioturbation diffusion coefficient decay with depth

Thus, the diffusivity coefficient, k_z, becomes the sum of the molecular and bioturbation diffusion coefficients:

$$K_z = D_m + D_b$$

3.5.6.3. Particulate properties

Particulate properties ($kg_{property}/kg_{sediment}$) vary in time due to sinks and sources, namely adsorption/desorption, and due to bioturbation mixing effect.

$$\frac{\partial (C_p)}{\partial t} = \frac{\partial}{\partial z}(D_b \frac{\partial C_p}{\partial z}) + (Sources - Sinks)$$

3.5.6.4. Adsorption/Desorption

Adsorption and desorption processes are simulated with a similar approach as in the water column.

4 MODEL CALIBRATION AND TEST CASES

4.1. Test cases setup

This chapter describes some test cases regarding new processes included in the model. Several setups were made in order to isolate the processes whished to calibrate, identified in each of the following sub-chapters.

Calibration was carried out to analyse the model response to several parameterizations, before applying it to a full realistic application, where it is more difficult to assess the relative importance of a specific process.

In order to test the model under various conditions, in a way that, simulations would be fast to run but still using realistic forcing, MOHID was executed using the 1D vertical mode, which is a specific option and an example of the model's versatility. This mode enables to force the model with a surface shear stress that develops a velocity profile. This surface shear stress can be imposed by a cyclic time series, with a semi-diurnal period, therefore resulting in a bottom shear stress variation (Figure 13) similar to a semi-diurnal tidal flow. This is useful to simulate bottom shear stress dynamics, the governing process of erosion and deposition.

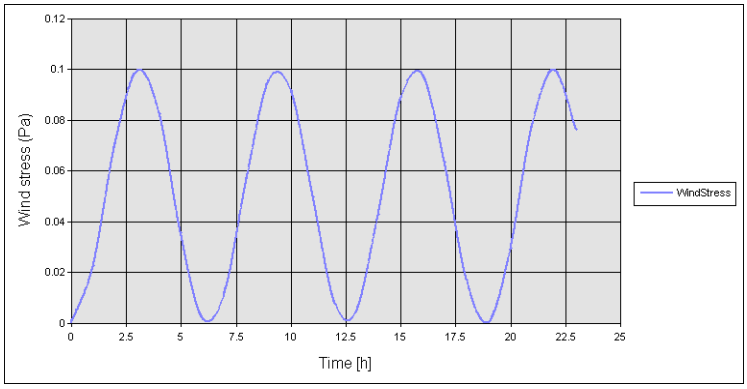

Figure 12 – Imposed wind stress cyclic time series with a semi-diurnal period

Null gradient lateral boundary conditions are considered at all times. In all tests the model was setup with a 10m layer in the water column and a 20cm sediment compartment, divided into 50 equally spaced layers, being the upper 10 layers left empty (to account for possible creation of new layers due to consolidation).

4.2. Erosion

Erosion and deposition processes were already implemented into the model, but were only applied at the fluff layer. This meant that when the fluff layer was totally eroded, erosion stopped. However, as described before, depth dependent differential erosion rates were included and the new algorithm for the sediment vertical coordinate needed to be tested. This is one of the key processes implemented in the model, as it is possible to collapse control volumes, allowing to compute the vertical sediment column with a variable number of layers during run-time. In the "empty" layers, sediment and interstitial water volumes are set to zero, as well as properties concentrations. This is accomplished, as defined in the previous chapter, by a mass conserving algorithm that attaches and detaches two layers as minimum and maximum thicknesses are reached.

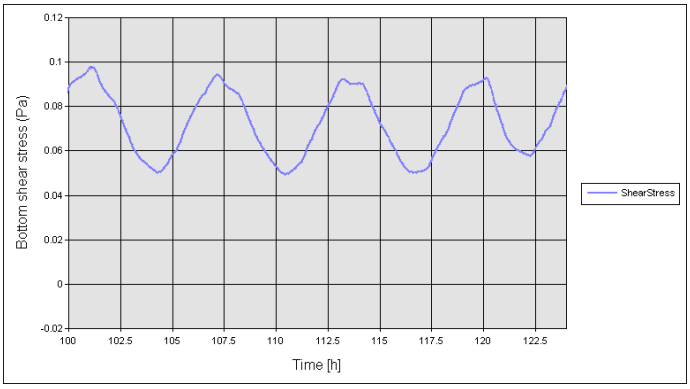

Figure 13 - Bottom shear stresses obtained from the 1D vertical model during 1 day

In order to test this feature, taking into account the computed bottom shear stresses (Figure 13), ranging from 0.05 to 0.1 Pa, critical shear stresses for erosion were defined in a way that erosion would occur most of the time (Figure 14). Thus, a critical shear stress of 0.02 Pa was defined at the upper layer with an exponential increase to 0.2 Pa in the lower layers.

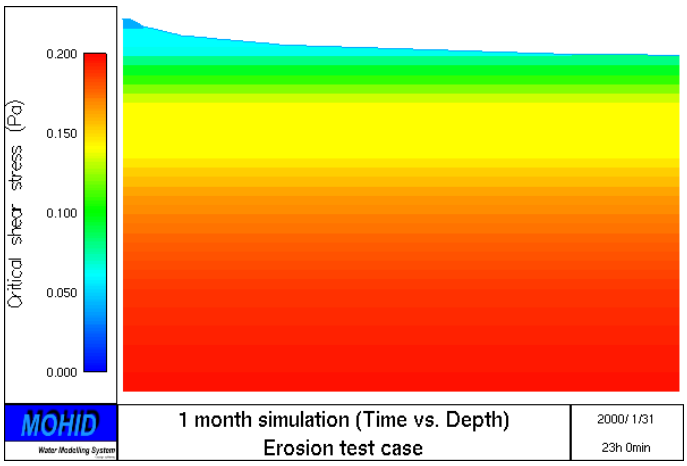

Figure 14 - Top layers collapsing in erosion test case

Results are purely illustrative of the way top sediment layers collapse as they reach minimum thickness allowed, in this case 1mm (Figure 15).

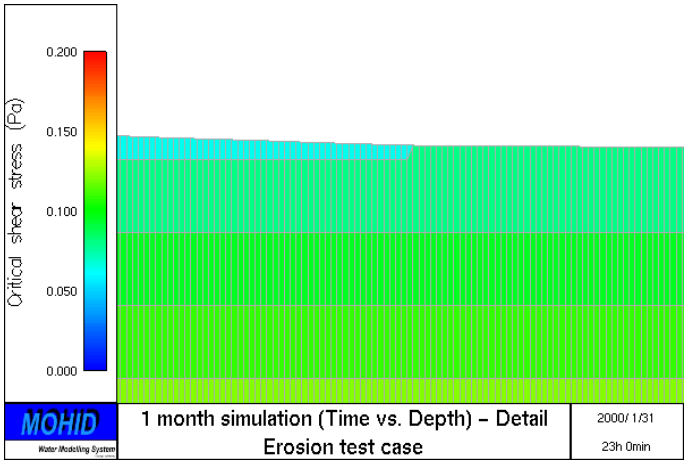

Figure 15 - Detail of collapsing layer in erosion test case

Also, as described before, erosion occurring from the sediment compartment results in a flux of interstitial water to the water column. With this flux, solutes present in interstitial water are also flushed. A simple test case is presented, in which the sediment interstitial water was initialized with constant conservative tracer concentration (1 mg/l) and the water column with null tracer concentration and null SPM concentration. Porosity in the sediment was considered 0.5. Thus, for each sediment control volume, half is water and the other half is dry sediment. This way, in terms of the control volume and considering sediment dry density equal to 2300 kg_{sed}/m^3sed, the "concentration" ratio between sediment and the dissolved tracer will be $2.3x10^6$, being this ratio maintained in the water column as erosion takes place (Figure 16).

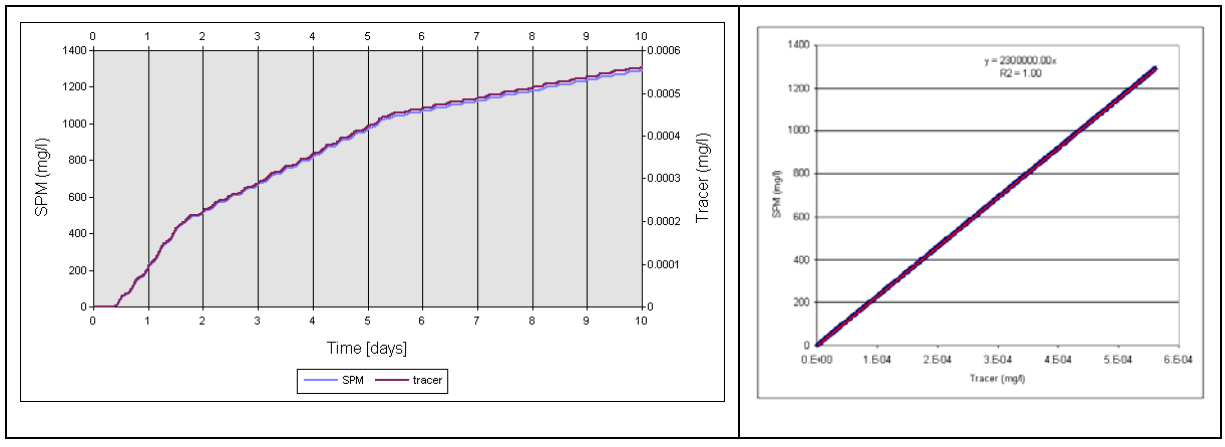

Figure 16 - Erosion of a tracer dissolved in interstitial water. SPM and tracer concentrations in the water column (on the left) and ratio between them (on the right).

4.3. Consolidation

Fluff layer consolidation rates are simulated as a decay of sediment deposited mass from the fluff layer to the consolidated sediment compartment upper layer. To get a hold of the range of values that can be used as consolidation rates and represent the order of consolidation time scale, in Figure 17 is presented the relation between consolidation rates and the time needed for 90% of the initial mass to get consolidated and enter the sediment compartment.

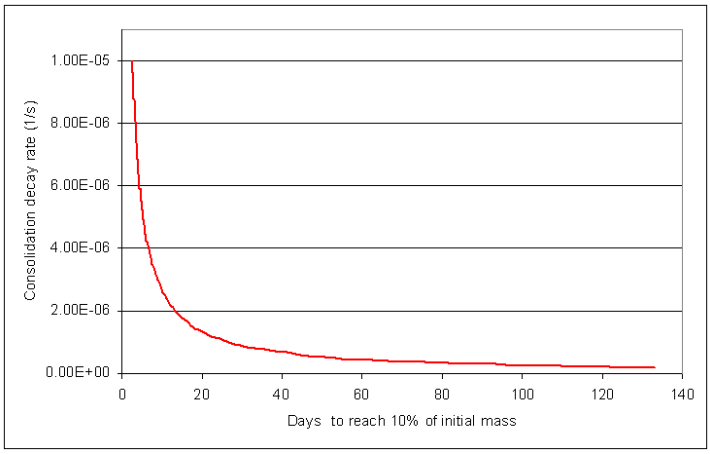

Figure 17 - Consolidation decay rates vs. Time to reach 10% of initial mass

To test consolidation in the model, hydrodynamic forcing was disconnected and the water column was initialized with a high suspended matter concentration (1g/l). The suspended particles settle on the bottom and, as bottom shear stresses are null, these recently deposited sediments are progressively being consolidated into the sediment compartment. Different rates of consolidation were used, during 1 month simulations, and compared in terms of gain for the sediment compartment (Figure 18).

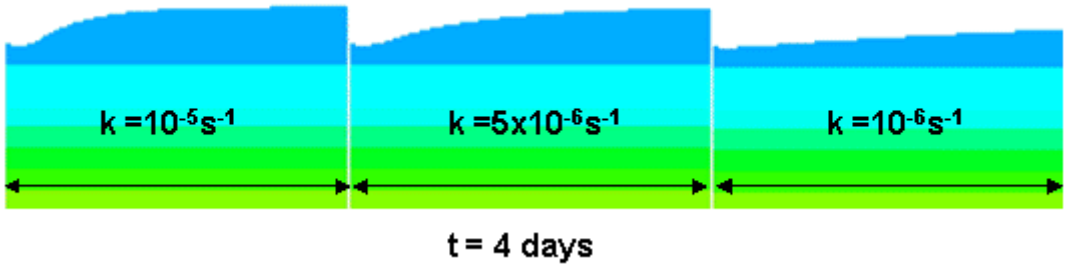

Figure 18 - Comparison between different consolidation rates

Maximum thickness was defined to have 6 mm, after which a new layer is created (Figure 19).

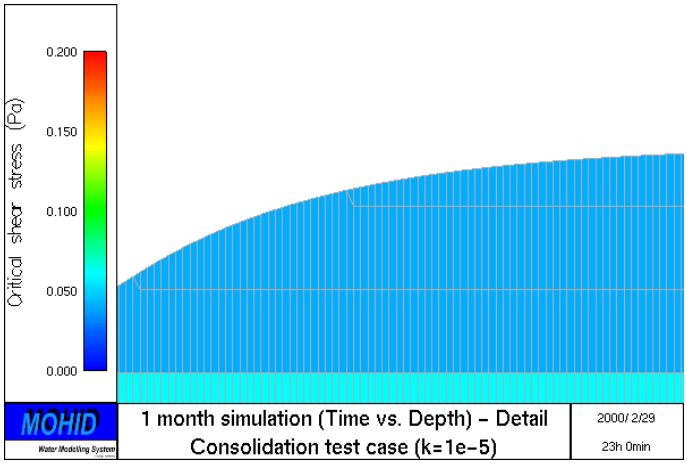

Figure 19 - Detail of the creation of a new layer due to consolidation

When consolidation occurs, water over the sediment bed is dragged along with the sediment, as well as solutes present in that water. The algorithm is the same used in the inverse process (erosion) and has been demonstrated in the previous chapter.

4.4. Adsorption-Desorption

Adsorption and desorption is modelled as a single reversible process. It is considered that the kinetics of the adsorption reaction is equal to desorption, in the form of a kinetic rate. This rate defines the time scale in which equilibrium is reached, and can be obtained from laboratory studies. Nevertheless, it is necessary to understand the relative importance of this parameter in contaminants distribution.

Let us consider a schematic situation of a contaminant in an estuarine water column, in which equilibrium ratio defines that 90% of a contaminant is adsorbed onto suspended particulate matter. If at a certain instant, equilibrium is broke and dissolved and particulate concentrations are equal, one can compute the time necessary to resume equilibrium.

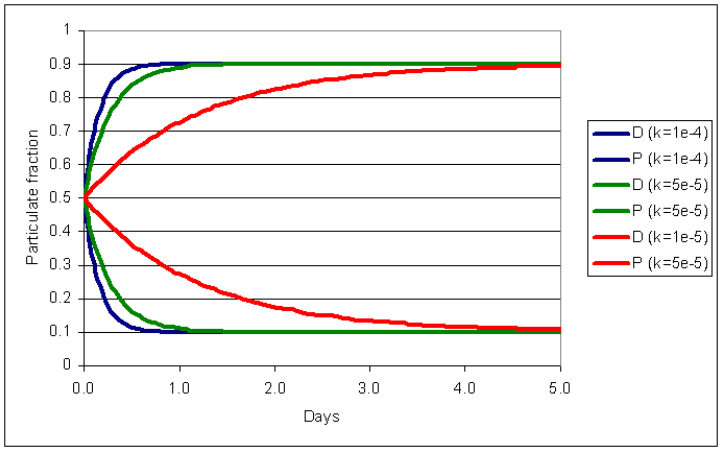

Figure 20 - Sensitivity analisys on the partition kinetic rate

Ranging values from 10^{-4} and 10^{-5} s, time scales to resume equilibrium vary from 0.5 to 4 days. If the kinetic rate of a contaminant is high and the time scale of equilibrium becomes near the time scale of, for example, the tide or erosion/deposition processes, then it becomes also a governing process. This is due to the fact that it highly affects contaminants' concentration variation, therefore controlling its distribution in the water column. This can be observed in the following test: assuming a sinusoidal variation of the particulate phase, with an approximate 12 hour period, representative, for example, of the effect of its deposition and resuspension (Figure 21).

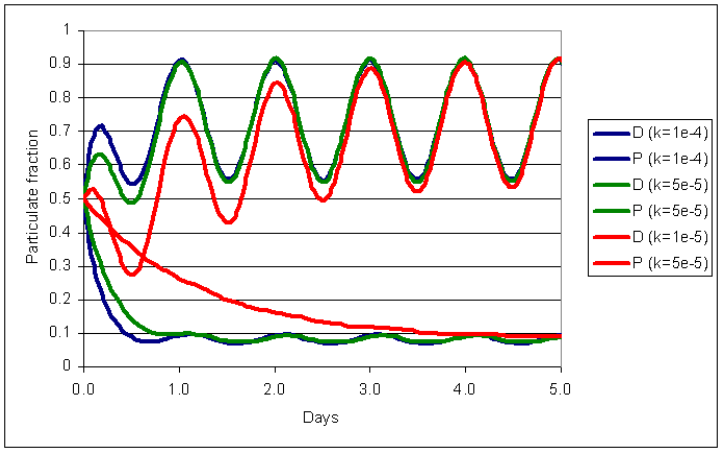

Figure 21 - Sensitivity analisys on the partition kinetic rate assuming an imposed variation on the particulate phase

In this case, with higher kinetic rates, the dissolved phase presents a visible sinusoidal variation caused by the imposed variation of the particulate phase; a variation which is imperceptible with lower kinetic rates.

5 MODELLING ARSENIC DYNAMICS IN THE TAGUS ESTUARY

5.1. Overview

The Tagus estuary is the largest Portuguese estuary and one of the largest in Europe. It is located near Lisbon and covering an area of about 300 km^2 at low tide and 340 km^2 at extreme high tide (Vale and Sundby, 1987). The estuary can be divided into 3 main areas: a straight and narrow W-E oriented seawater inlet channel about 16km long, 2 km wide and reaching 40m depths; a shallow inner bay 25km long, 15km wide with a SW-NE orientation; and the Tagus river entrance composed of several shallow channels in the North of the estuary. There are 3 main affluent rivers: the Tagus, Sorraia and Trancão. The Tagus River is the most important fresh water tributary in the estuary. Its discharge has a pronounced seasonal variability, with flow rates varying typically between 50 and 2000 m^3/s. Sorraia and Trancão have a mean discharge of 39m^3/s and 6m^3/s, respectively.

Tagus estuary is a semi-diurnal mesotidal estuary, varying from 1m neap tides to almost 4m spring tides. The tidal excursion is almost 80km landward of Lisbon, and at spring tide the

high water is delayed by as much as two hours between Lisbon and Vila Franca de Xira. The mean residence time is of about 25 days (Braunschweig et al., 2003).

Lisbon's metropolitan area, composed of about 2.5 million people is located around the estuary. Only the Northeast area of the estuary is protected and consists of a natural reserve with high biodiversity and a nursery zone for several species of molluscs, migrating fish and birds, and is constituted by extensive salt marshes.

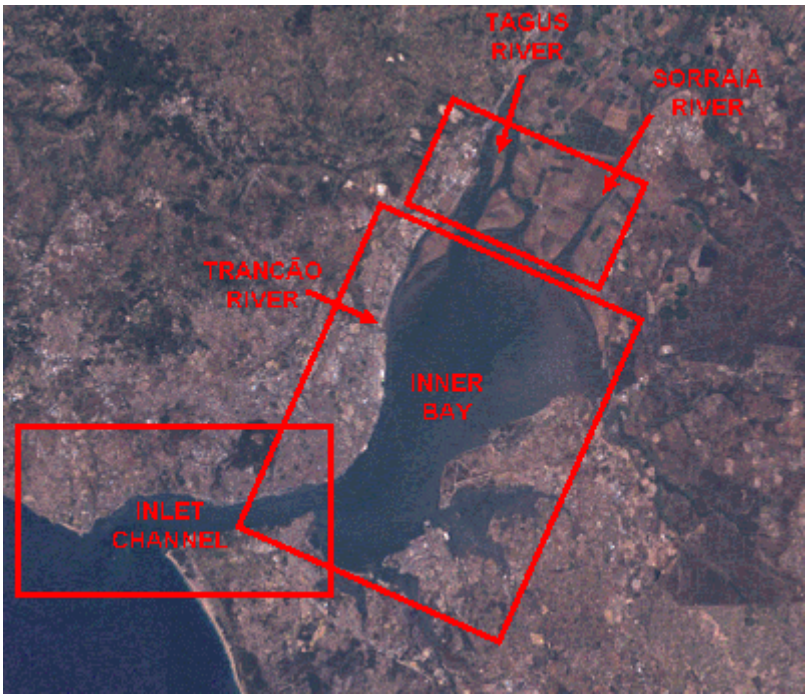

Figure 22 – Tagus estuary

Generally speaking, the estuary has suffered anthropogenic pressure from agriculture, animal explorations, fisheries, urban wastes and mostly from industry. Since the industrial revolution, hard industry set base on the estuary margins, due to the proximity of Lisbon. The Southeast margins of the estuary were occupied by a large number of industries, namely the Quimigal pyrite processing unit near Barreiro (Figure 23), which worked from 1960 until 1986-87.

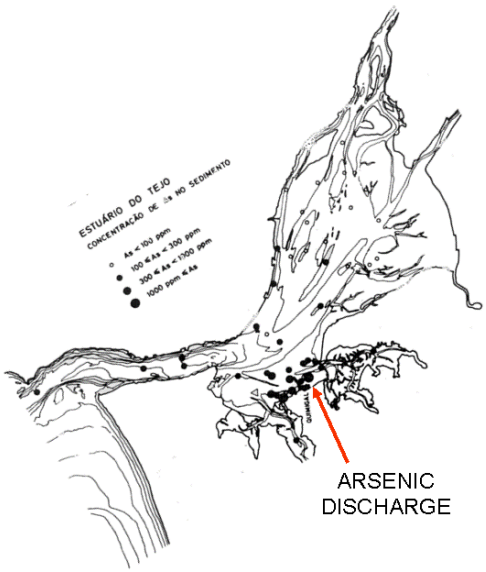

Figure 23 - Superficial sediment total arsenic concentrations (reproduced from Bettencourt, 1990)

In this plant, about 7.900.000 tons of pyrite were processed during 36 years. Assuming a content of arsenic of about 0.52% (EUROSSAM, 2000), it is estimated that about 700 to 1100 tons of arsenic per year reached the estuary from smelter operation. These values take into consideration the liquid effluent, as well as, atmospheric emissions, and consequent particle deposition on the estuary and on the local watershed with consequent run-off to estuarine waters.

5.1.1. Arsenic estuarine biogeochemistry

The spatial and temporal speciation of arsenic depends on chemical processes, namely in changes on redox conditions and also on biological processes, such as, uptake by phytoplanktonic communities.

The predominant form of inorganic arsenic in estuaries is arsenate. Arsenite, the reduced inorganic fraction, and two methylated forms, monometilarsenic (MMA) and dimetilarsenic (DMA) can also be found. Other, more complex, forms can also be found but in very small quantities, undetectable when using the most common methods.

Arsenate, due to the similarities to phosphate, is consumed by autotrophic organisms together with it, therefore interfering with phosphate main functions inside the cell, namely the oxidative phosphorilation and TPA production. Thus, when the arsenate/phosphate

ratio is relatively high, arsenate toxicity to phytoplankton is likely to occur (Sanders et al, 1994).

Arsenite is the most stable inorganic form in reductive environments, such as anoxic water or sediments. However this predominance is likely to be affected by biological activity (Bettencourt, 1990). The methylated species are produced biologically by methylation of inorganic arsenic and by the degradation of arsenic organic compounds such as arsenocoline or arsenobetaine (Hanaoka et al, 1987 in Sanders et al, 1994).

Arsenic toxicity can vary in several orders of magnitude, depending essentially on its speciation. Toxicity levels of arsenic organic compounds are, generally, lower than the inorganic forms (Bettencourt, 1990). Studies performed in areas with high level sediment contamination with arsenic, and by other metals, showed significant reductions in polichaete, bivalve and crustacean populations (Clark, 1997 in Portela, 1997), representing the effect of a contaminant with a primary impact in the beginning of the trophic chain, with a cascade effect to the superior levels.

5.1.2. Arsenic partitioning

Andreae et al (1983) performed a number of arsenic measurements in the Tagus estuary, in which dissolved and adsorbed concentrations were obtained. The samples were obtained at a time the smelter was still operating. From these results, partition coefficients in the water column were derived (Figure 24), with adsorbed fractions ranging from 25% to 75% of total arsenic.

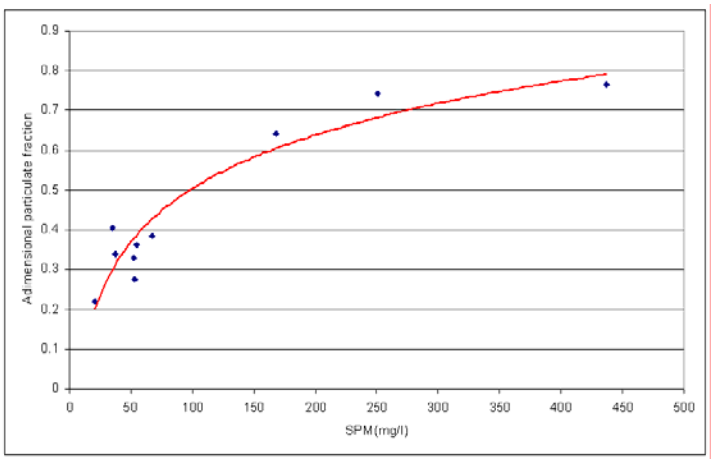

Figure 24 – Relation between suspended particulate matter and the particulate fraction (Data derived from Andreae, 1983)

A dependence of this distribution with suspended particulate matter (SPM) corroborates with the fact that higher adsorbed concentrations are found in maximum SPM concentrations areas, which indicates that adsorption probability increases with increasing particulate matter concentrations. Thus, the formulation proposed for adsorption-desorption kinetic rates, relating it with SPM can be accepted. Nevertheless, a relative uncertainty is found in defining the reference kinetic rates, which can be obtained in laboratory studies. In this study, a value of $5e^{-5}$ s was considered.

In the sediment compartment, equilibrium conditions are quite different from the water column. Martin et al (1982) and Bettencourt (1990) found superficial sediment concentrations of arsenic adsorbed phase in the range of 1 ppm in uncontaminated areas reaching 400ppm (Martin, 1982) and even 3000ppm (Bettencourt, 1990), near the Quimigal discharge (Figure 23). Measurements of both adsorbed and dissolved arsenic phases are scarce, both in the Tagus estuary and in literature. This is, generally speaking, due to the difficulty, not only logistic of obtaining the samples, but also technical, in measuring porewater concentrations.

Fabian et al. (2003) performed an extensive study in Lake Balderggersee, in Switzerland, where vertical profiles of adsorbed and dissolved arsenic phase were measured, being the observed order of magnitude of dissolved concentrations around 20 ppb and with adsorbed concentrations reaching up to 60 ppm. Although contaminant transport processes in lakes are quite different from estuaries, it was considered that the relationship between the two phases is illustrative of the overwhelming affinity of arsenic to adsorb on to the sediment bed, under the specific conditions of the benthic compartment. Thus, an overall particulate fraction of 99.9% can be considered in the sediments.

5.2. Results

The Tagus estuary is considered to be the reference modelling system for MOHID Water. Is has been modelled extensively with MOHID (e.g. Portela, 1996; Pina, 2001; INAG, 2002; Leitão, 2003; Braunschweig et al, 2003; Pina et al, 2004). Recently, an operational setup of the model has been made enabling hydrodynamic and water quality forecasts for the Tagus estuarine region (http://www.mohid.com/tejo-op/).

5.2.1. Hydrodynamics

MOHID hydrodynamic model has been widely applied to the Tagus estuary, therefore in this study, only some characteristic results are presented, in order to complete the description of the estuary. The model was setup on a 91x105 cells grid (Figure 25), with a non-constant spacing resolution, varying from 2000m at the ocean open boundary and progressively reducing into the estuary where a 500m resolution is obtained.

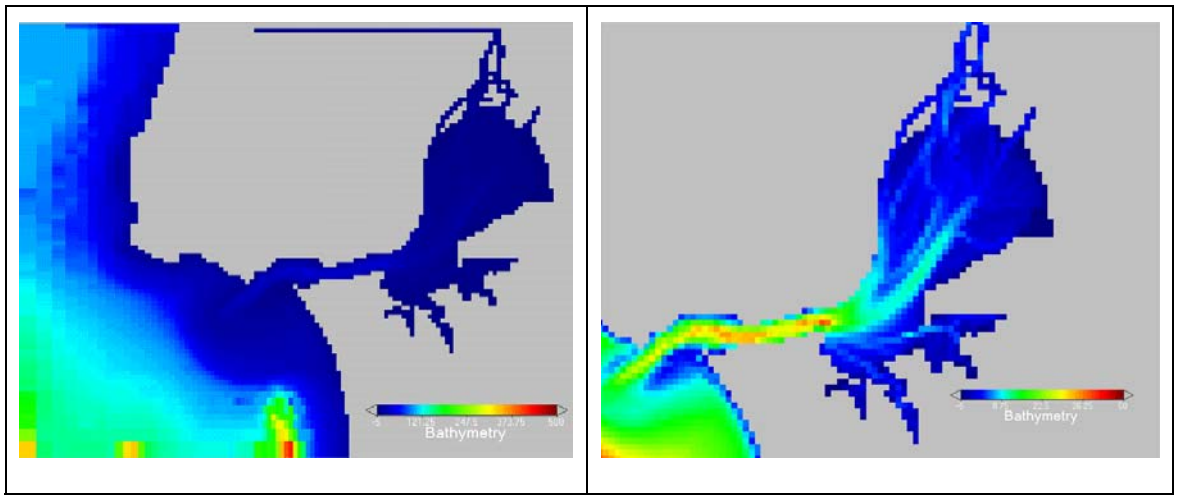

Figure 25 – Tagus estuary bathymetry over the variable resolution grid.

The Tagus river discharge was set to a constant value of 300 m^3/s (mean annual discharge), in all simulations, as well as Sorraia river (39 m^3/s). Tide was imposed at the open boundary, based on harmonic components obtained with a global tide solution model (Le Provost et al, 1998). The model was setup in vertically integrated mode, and baroclinic and atmospheric forcing were switched off. This approach pretends to simulate strictly tidal induced flows with mean river discharge conditions, which are the most important hydrodynamic processes prevailing in the framework of this study.

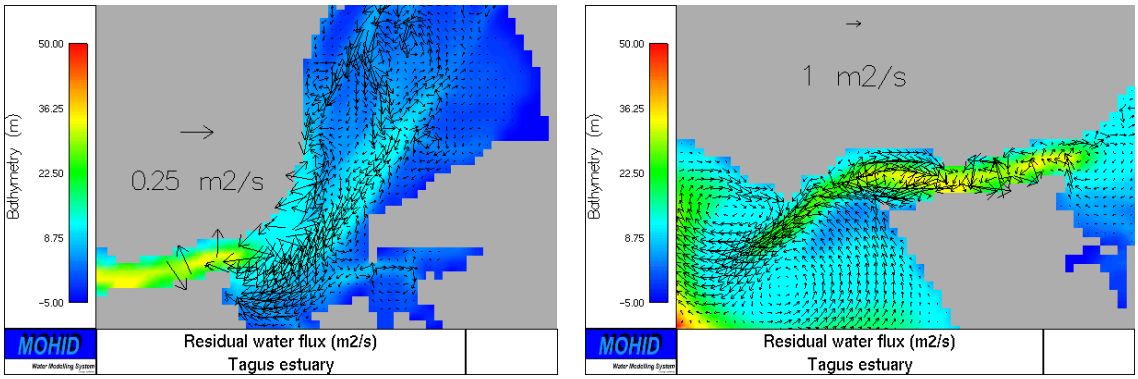

Figure 26 – Residual water fluxes (m^2/s) inside the estuary (left) and in the mouth of the estuary (right)

Figure 26 presents the residual barotropic water fluxes (residual velocities multiplied by depth) in the estuary after a spring-neap tide cycle (Figure 27). In the right hand side figure an intense recirculation can be observed on the estuary's mouth, with water exiting the estuary from the main channel, re-entering through the margins.

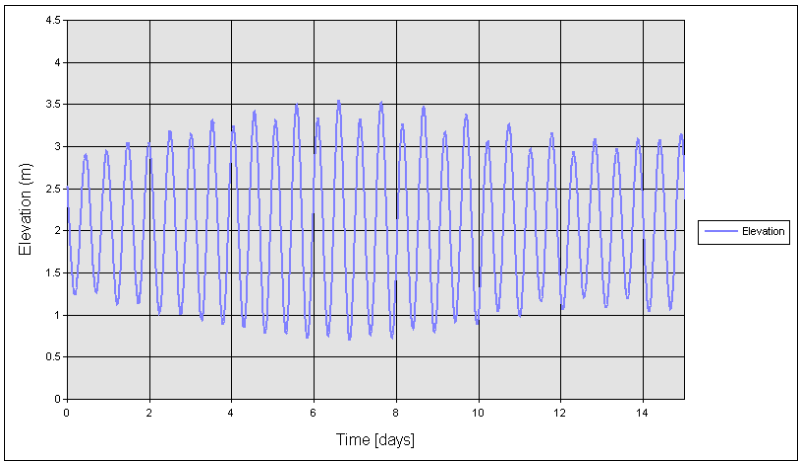

Figure 27 - Water elevations in the Tagus estuary main channel (Spring-neap tide cycle)

Below are shown (Figure 28), in an illustrative way, the velocity fields for flood and ebb during a spring tide.

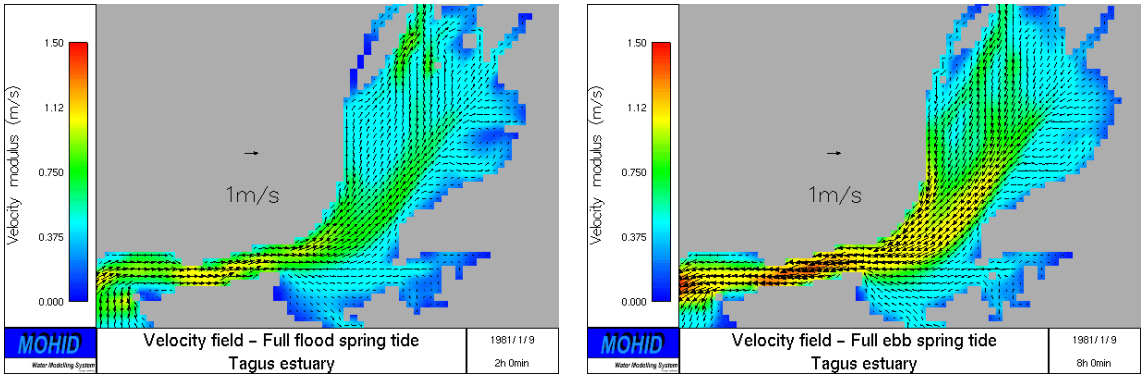

Figure 28 - Velocity fields for flood and ebb during a spring tide

5.2.2. Cohesive sediment transport

Due to the integration of the sediment compartment model in MOHID, a new methodology to simulate cohesive sediment transport in the Tagus estuary was developed. Cohesive sediment transport modelling depends on a small amount of parameters, such as settling velocity, critical shear limits for erosion and deposition to occur and a reference erosion rate. These parameters are highly variable, depending on sediment grain size and composition, and literature, as demonstrated in previous chapters, provides a wide range of variation for them. Thus, some calibration is needed. Previous methodologies were based on a single fluff layer model, which, starting with a uniform sediment distribution at the bottom of the estuary, the model would be run and sediment would be eroded from the areas where high bottom shear stress values occur, and would deposit in calm zones. Each grid cell would have its own parameterization (normally assumed constant in the domain) and after the fluff layer was entirely eroded, erosion would stop. This resulted in a more or less stabilized sediment distribution map which could afterwards be used as an initial condition for model simulations.

The new methodology is based also on the fluff layer model, but only to account for the recently deposited sediments. A warm-up run is also made, but this time, defining an initial empty fluff layer, and below a sediment compartment with several layers. Each layer has a different critical shear stress for erosion to occur, increasing with depth. Thus, erosion rates will decrease in time as sediment upper layers are being scoured and erosion occurs at increasing depths. The warm-up simulations final result is a map, not of sediment distribution, but of critical shear stresses for erosion to occur. This methodology is believed

to constitute an improvement in the definition of the initial bottom sediments distribution, therefore benefiting cohesive sediments transport solutions and finally contaminant transport modelling.

5.2.2.1. Warm-up simulation

The Tagus and the Sorraia Rivers discharges were defined with a constant concentration of 100 mg/l (Portela, 1996; Pina, 2001), and the water column initial condition was obtained after a short warm-up simulation.

The consolidated sediment compartment was defined with 20 cm depth, below the entire water column, divided into 15 layers, being the upper 5 left empty to account for consolidation. Minimum and maximum layer thicknesses were setup to 1mm and 50mm respectively. Based in Portela (1996), critical shear stresses for deposition and erosion were considered to be 0.2 N/m^2 and 0.4 N/m^2, respectively. The same values were used in the fluff layer. In the sediments' upper layer, a value of 0.5 N/m^2 was defined with an exponential increase with depth (Figure 29). In the empty layers above, an upward decay from 0.5 to 0.4 N/m^2 was considered, to account for newly created layers, due to consolidation, having lower shear strength.

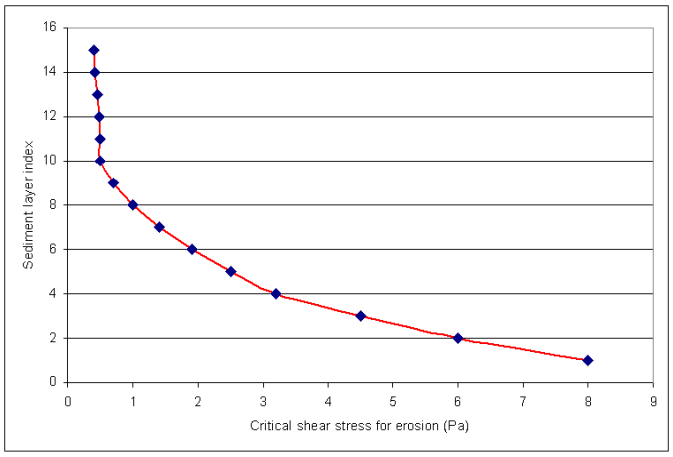

Figure 29 - Critical shear stress for erosion increase with depth (Higher indexes refer to upper sediment layers)

The model was run during 3 spring-neap tide cycles, after which a final map of critical shear stresses was obtained.

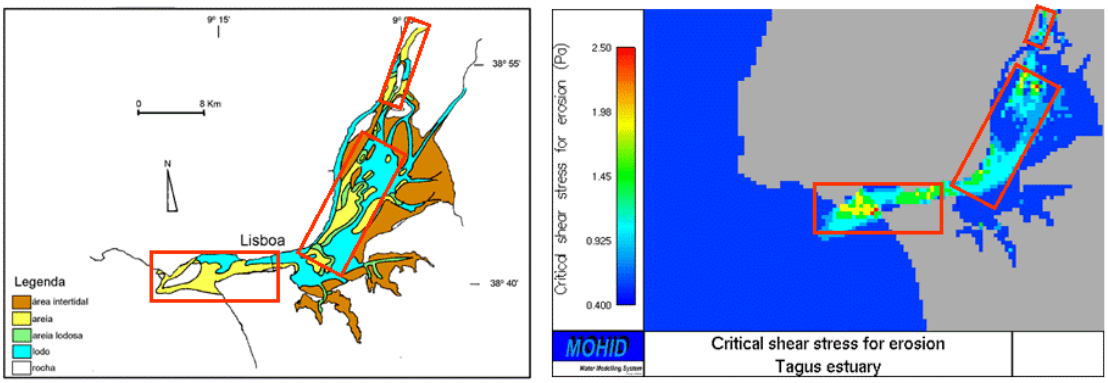

Figure 30 - Sediment characterization of the Tagus estuary (adapted from Calvário, 1982, in Garcia, 1997) on the left (Yellow zones – sand; brown zones – intertidal areas; cyan zones – mud; green zones- sand and mud). On the right model critical shear stress for erosion distribution after 3 spring-neap tide cycles.

Results show that erosion occurs in the estuary's mouth channel and along the inner estuary's main flow axis, where higher velocities are present. Comparing this map with the distribution of sediment classes, in terms of size and composition (Figure 30), a good relation between sandy sites and high values of critical shear stresses can be obtained. Thus, a first conception of fine sediments' fate can be drawn, and ultimately the distribution of arsenic in the Tagus sediments.

5.2.2.2. Validation

Deriving the critical shear stresses for erosion from the warm-up simulation, spring-neap tide simulations were performed to validate cohesive sediment transport in the Tagus estuary. Complementary, simulations including the effect of wave induced bottom shear stress were executed as means of comparison and to assess the importance of local waves in the Tagus estuary. As the estuary is about 20km wide, given the correct alignment of the wind, which is predominant from N-NE, waves can be generated with higher probability in the Eastern areas of the estuary, mostly composed of intertidal mudflats, and therefore influence the deposition and resuspension processes there. Thus in these areas, constant values of wave period (3 s) and wave height (15 cm) were considered.

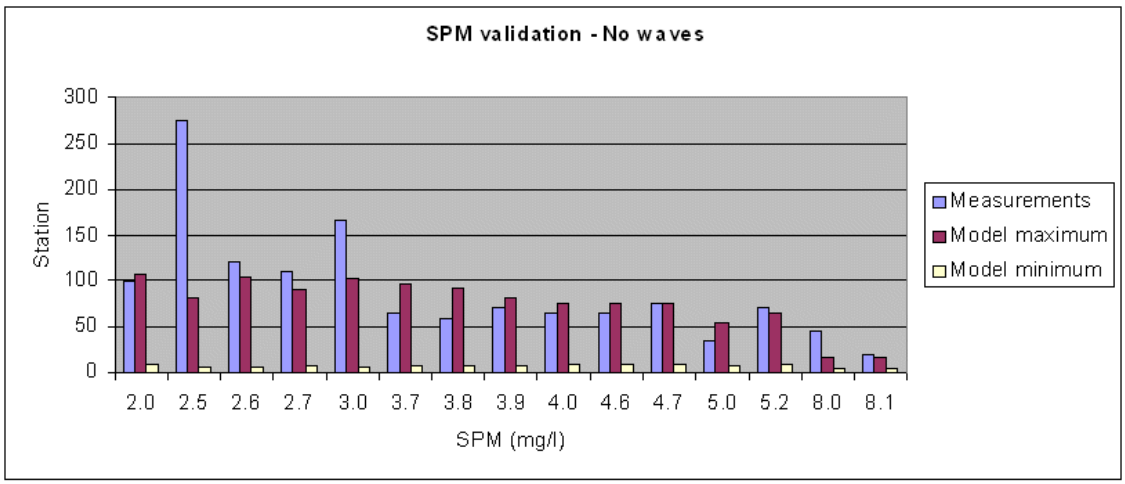

Figure 31 – Cohesive sediment model results comparison against measurements. Scenario without waves

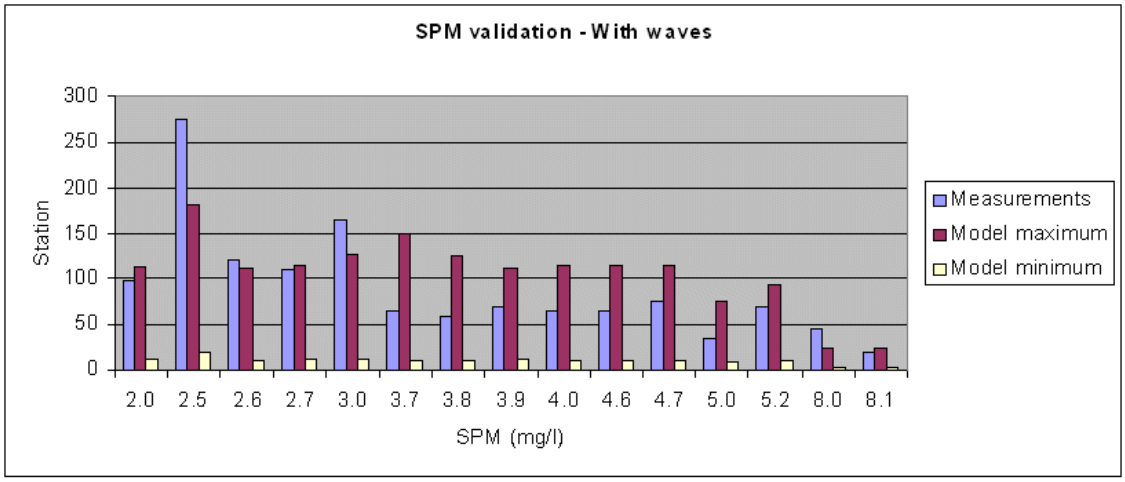

Figure 32 - Cohesive sediment model results comparison against measurements. Scenario with waves

Figure 31 and Figure 32 present a comparison of modelled minimum and maximum concentrations over a spring-neap tide cycle against historical measurements collected in the estuary (in Pina, 2001). Stations locations are presented in Figure 33.

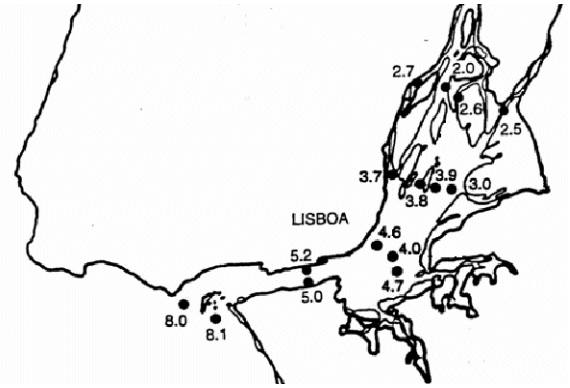

Figure 33 - SPM stations locations

Model results show good agreement with the field data, except for field stations 2.5 and 3.0, located in the intertidal NE areas of the estuary, more susceptible to waves' action, as explained before. This is clearer when comparing with model results including waves' influence, as model results are improved (Figure 34). It is probable that with the correct wave parameterization, model results improve even more, leading to a possible coupling of MOHID with a wave model. Nevertheless, an overall good agreement can be provided.

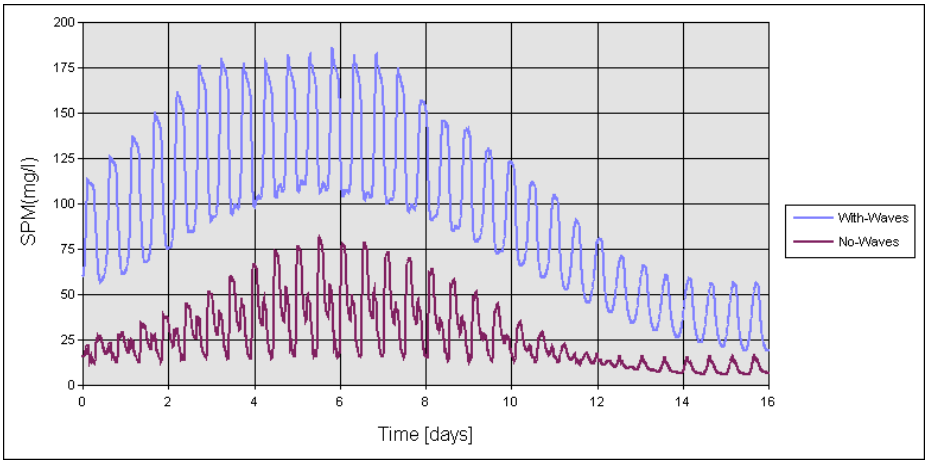

Figure 34 - Comparison of model results, between scenarios with and without waves over a spring-neap tide cycle in station 2.5

5.2.3. Lagrangian tracers

The first approach to study the arsenic discharge of the Quimigal plant was using lagrangian tracers, in order to assess the main deposition zones where contaminated sediment particles

will settle. Several particle diameters, Figure 35, were considered within the cohesive sediment range (<64μm), to account for differential settling.

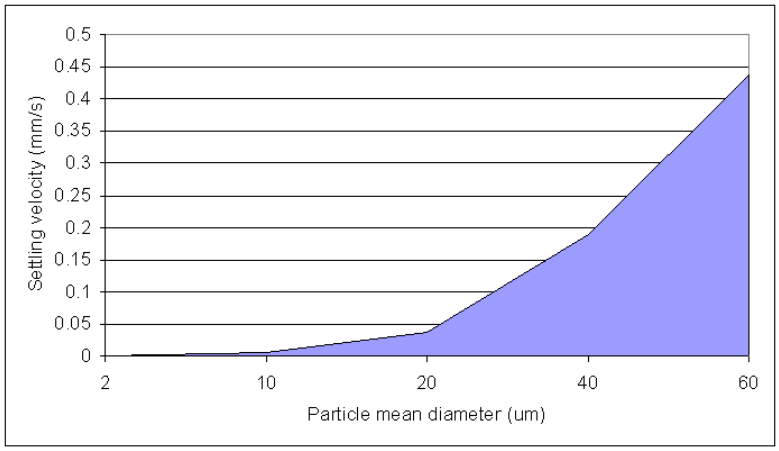

Figure 35 – Lagrangian tracers' particles diameters and correspondent estimated settling velocities

The model was again executed through a spring-neap tide cycle, with a continuous particle emission (1 particle per diameter class per time step). The intent of this simulation is not to define different deposition zones for different particle sizes, but to, define overall cohesive sediment deposition zones. This methodology, considering, that the arsenic distribution in the particulate phase is independent of particle size within the 64 μm range, allows the delimitation of areas most probable to become contaminated with arsenic in the sediment compartment. Results (Figure 36) clearly demonstrate that sediment particles tend to deposit extensively in the adjacent areas of the discharge and along the South East channels of the estuary.

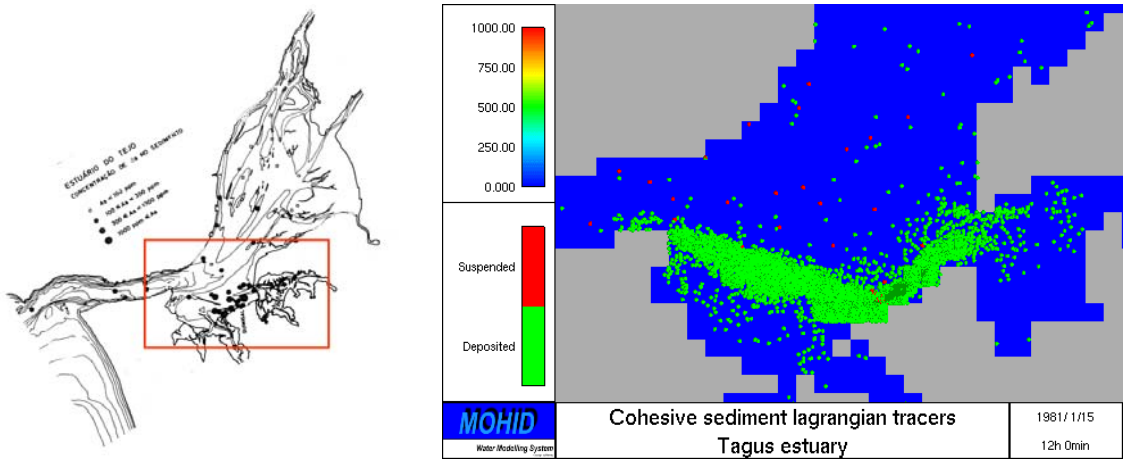

Figure 36 – Comparison between measured arsenic concentrations in superficial sediments (on the left) and sediment lagrangian tracers' position after continuous emission over a spring-neap tide cycle (on the right). Particles in green colour are deposited on the bottom, and particles in red are suspended.

The figures below (Figure 37) show the deposited and suspended particles in a full ebb situation during spring tide (figures correspond to the same instant but are shown separately to avoid graphical overlaying). This is the maximum velocity situation in the Tagus estuary and still most particles tend to remain deposited in the bottom, therefore reinforcing the idea that an important fraction of arsenic is retained in these areas.

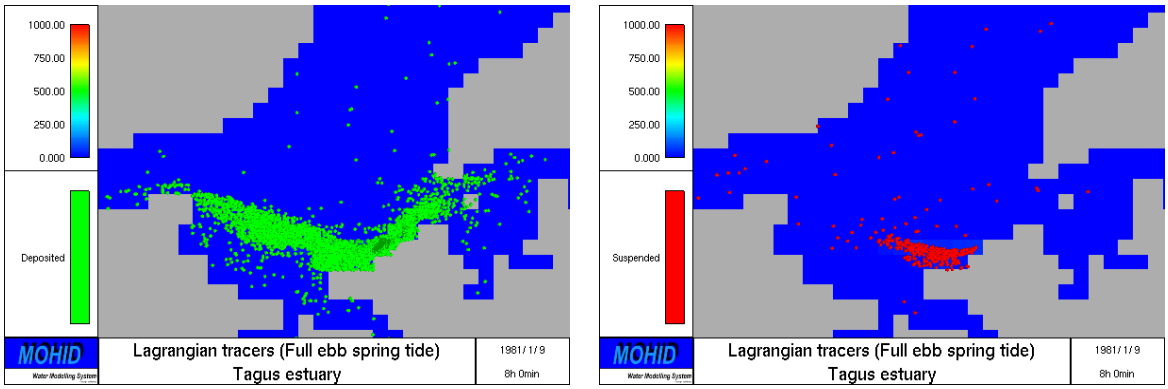

Figure 37 – Deposited (left) and suspended (right) particles in a full ebb spring tide situation.

Model results corroborate with superficial sediment total arsenic concentrations found by Bettencourt (1990), reaching up to 3000ppm (Figure 23).

5.2.4. Arsenic transport

5.2.4.1. Inputs

Three input discharges were considered, namely the 2 main affluent rivers: Tagus and Sorraia, and the industrial plant effluent, being a partition coefficient of 50% assumed in all of them. The Quimigal effluent was considered to have 1m^3/s flow, and considering an input of 700 tons/year, a discharge concentration of about 10mg/l per phase (dissolved and particulate) was derived. In the river discharges, residual values of arsenic were assumed. Below, in Table 3, the values considered in each discharge are summarized.

Discharge	Flow(m3/s)	Total arsenic concentration(ppb)	Daily input(kg/day)
Tagus	300	0.5	12.5
Sorraia	39	0.5	1.7
Quimigal plant	1	20000	1900

Table 3 – Arsenic inputs to the Tagus estuary

5.2.4.2. Arsenic spatial distribution

The model was run with the above described setup, for a period of 3 years, to simulate the effect of decades of discharges. Below are presented some spatial distribution results of arsenic, both in the dissolved and adsorbed phases.

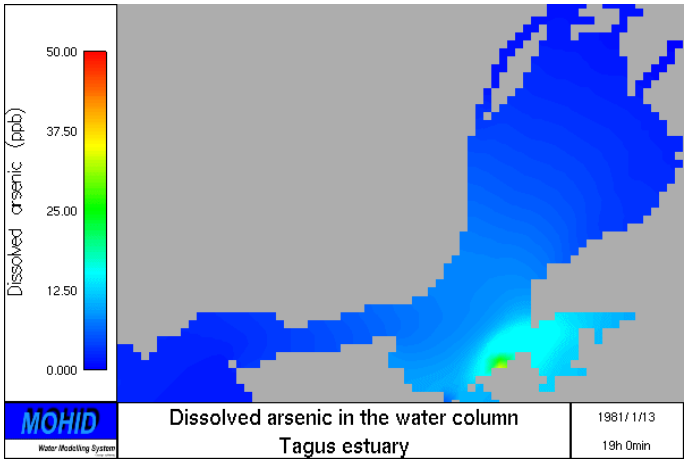

Figure 38 - Dissolved arsenic distribution in the Tagus estuary water column

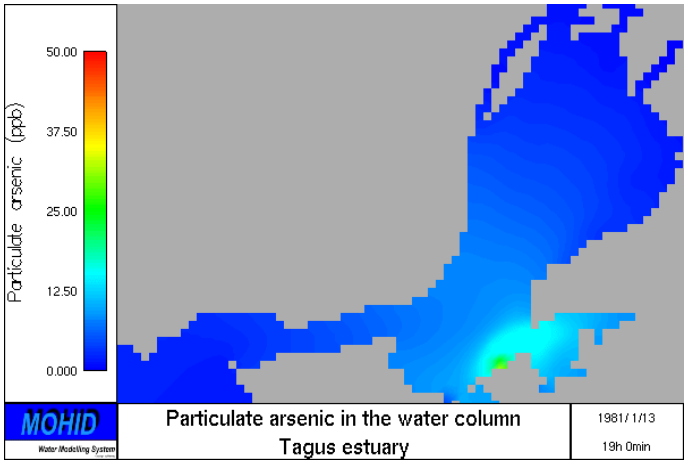

Figure 39 - Particulate arsenic distribution in the Tagus estuary water column

Figure 38 and Figure 39 represent the arsenic dissolved and particulate phases in the water column, during the effluent discharge. Higher concentrations are found near the location of the discharge, as expected, and a general dispersion is observed both in the estuary's inlet channel and in the main flow axis. In the Northern areas of the estuary, where Tagus River enters the estuary, and in the coastal areas outside, residual concentrations can be found.

As a partition coefficient of 50% distribution is assumed, one is lead to expect that (given the fact that the area near the discharge is a sediment deposition zone) a relevant fraction of the effluents' input is to be deposited in the sediment bed and remain there.

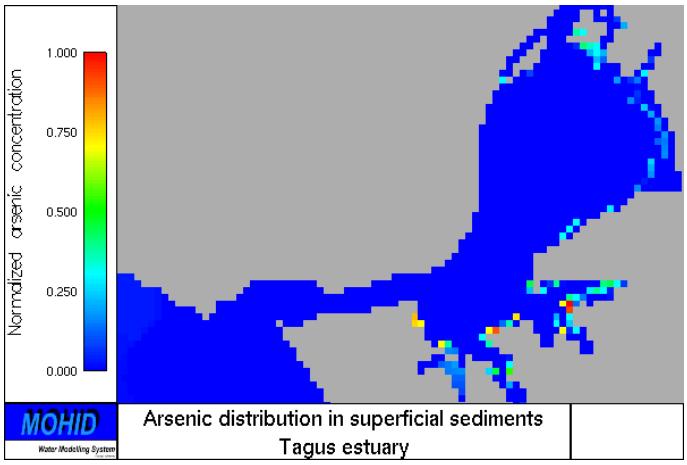

Figure 40 – Normalized arsenic distribution in superficial sediment

This is supported by model results (Figure 40), as maximum arsenic concentrations in superficial sediment are observed near the discharge. Nevertheless, due to transport inside

the estuary, one can observe that other peak concentrations are found in upper regions of the estuary, namely in deposition zones, therefore confirming the importance of hydrodynamics in the fate of estuarine contaminants.

A simple and straightforward way to describe arsenic dynamics in the Tagus estuary is to construct a conservative dilution curve, relating arsenic concentrations in the water column with salinity, a conservative tracer. This method allows indirect assessment of the spatial distribution of arsenic relating it with salinity, whose concentration presents a sharp gradient along the estuary's main flow axis, from the ocean influenced mouth salty waters to the up North fresh water area where the river meets the estuary.

Model results were compared with measurements taken contemporarily with the discharge Figure 41). Modelled values (dissolved arsenic concentrations and salinity) were obtained from several time series scattered along the estuary's main flow axis, during a spring-neap tide cycle. A good agreement is found with the measurements, therefore stating that the overall arsenic dynamics in the water column is resolved by model.

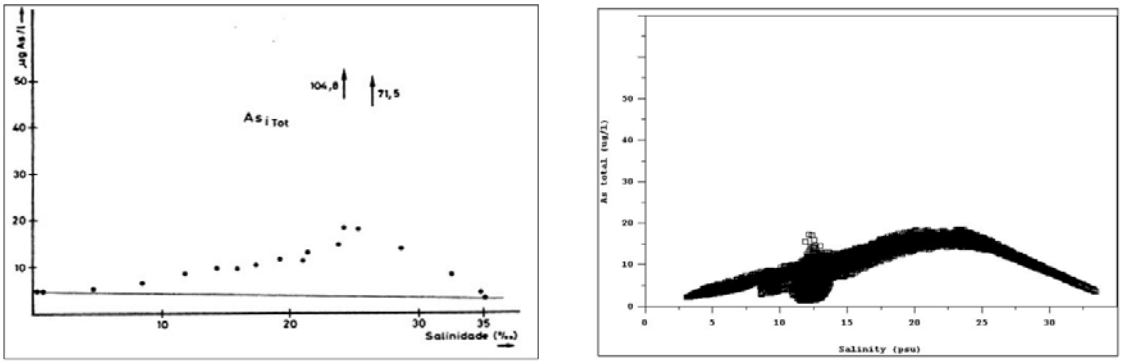

Figure 41 - Comparison of conservative dilution curves between measurements contemporary with the arsenic discharge and model results

As it is shown, there is an increase in arsenic concentrations near the 20-25 psu salt concentrations, which can be explained by the fact that these are the mean values of salinity near the point of emission. Model results present the same curvature, but some singularities can be observed also, as the number of "samples" taken by the model is much higher than the 10-20 samples taken in the field. Thus, higher variability is expected in model results. That is the case in the 10-15 psu region, located in the upper regions of the estuary, where maximum variability on suspended matter concentrations are observed, due to erosion and

deposition processes. This leads to an also high variability in the adsorbed arsenic concentrations, and ultimately in the dissolved phase, due to the partitioning hypothesis, through which the two phases tend to equilibrium concentrations given by a partition coefficient. Regard is made to the fact that maximum concentrations, both present in model and in measurements are out of the range of the graphics presented in Figure 41.

5.2.4.3. Arsenic sediment concentration profiles

In order to simulate the distribution of arsenic within the sediment column, some simulations were performed with the 1D vertical mode of the model. This was done to study the dynamics of arsenic in long term simulations. Thus, the model was setup as described in the calibration chapter considering two scenarios: a contamination scenario with high concentrations imposed in the water column and initial residual concentrations in the sediment column; and a no discharge scenario, with initial high arsenic concentrations in the sediment compartment and residual concentrations in the water column.

For the contamination situation, the worst case scenario was designed, performing 37 years simulations (approximately the period that the plant operated), and considering that the application zone of the 1D vertical model is a deposition zone located near the discharge. Thus, constant concentrations in the water column were maintained, by renewing the water column properties 4 times per day, considering adequate values from measurements taken at the time of the discharge: 20 ppb for both arsenic fractions, assuming a 50% distribution; and 100 mg/l of SPM, thus resulting in a particulate arsenic concentration of 200 ppm relatively to SPM. A constant SPM deposition rate was considered (10^{-5}g/m^{2}s), and different parameterizations for the bioturbation diffusion coefficient were compared. Nevertheless, the depth of bioturbation influence was kept constant in all simulations (10cm). Distribution in the sediment compartment was set to 99.9% adsorbed fractions. 50 sediment layers were also considered but this time with 30 empty layers, with porosity decreasing with depth (Figure 42).

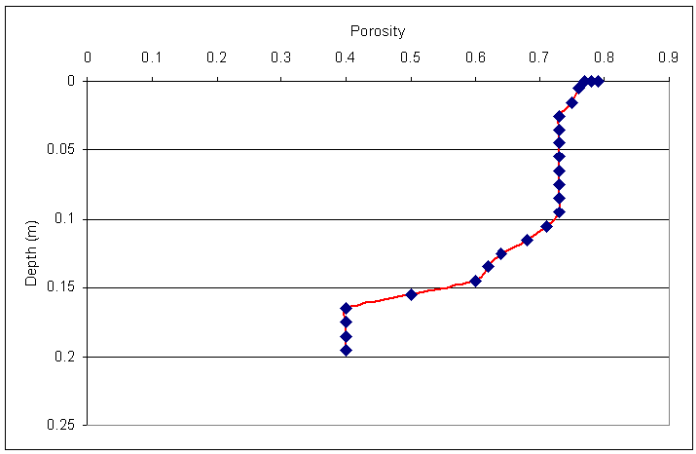

Figure 42 – Porosity profile considered in the simulations

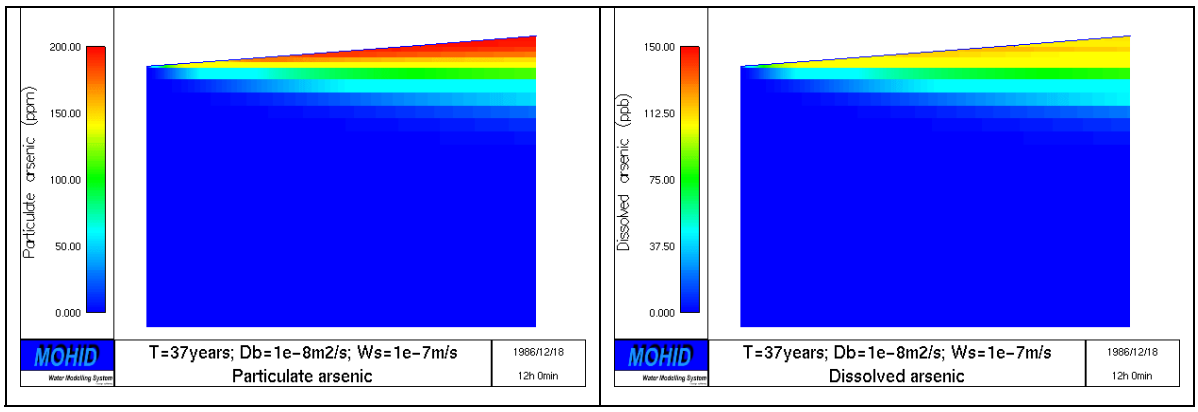

Figure 43 – Contamination scenario; Arsenic concentration profiles evolution (Time vs. Depth) during 37 years, with bioturbation coefficient = $10^{-8}m^2/s$ and SPM deposition flux = $10^{-5}g/m^2s$; Initial sediment thickness = 20cm

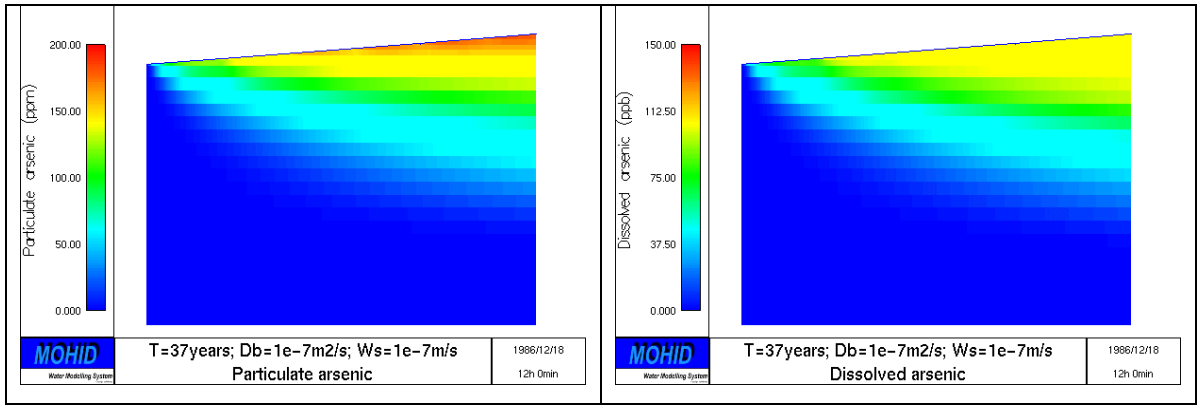

Figure 44 - Contamination scenario; Arsenic concentration profiles evolution (Time vs. Depth) during 37 years, with bioturbation coefficient = $10^{-7}m^2/s$ and SPM deposition flux = $10^{-5}g/m^2s$; Initial sediment thickness = 20cm

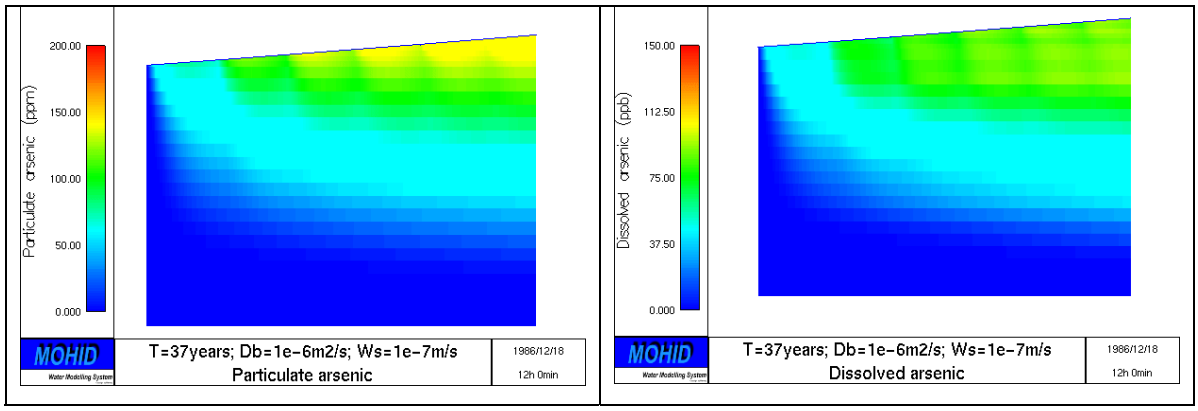

Figure 45 - Contamination scenario; Arsenic concentration profiles evolution (Time vs. Depth) during 37 years, with bioturbation coefficient = $10^{-6}m^2/s$ and SPM deposition flux = $10^{-5}g/m^2s$; Initial sediment thickness = 20cm

As expected, maximum adsorbed arsenic concentrations obtained in all simulations reached 200 ppm, which is the ratio prescribed in the water column. These concentrations are observed in superficial layers in all simulations, with exception made when using high bioturbation diffusion coefficients that tend to mix arsenic in the sediment column, transporting it to deeper layers. Interstitial water dissolved arsenic concentrations follow equilibrium concentrations defined by the partition coefficient, therefore presenting values near to 150 ppb. Here the same observations can be made regarding the bioturbation effect on its distribution. Bioturbation appears be to the governing mechanism to transport arsenic in the sediment column, as the higher the bioturbation effect is parameterized, the deeper arsenic penetrates in the sediment.

Another simulation was performed increasing the SPM deposition flux to $5x10^{-4}g/m^2s$, therefore introducing more contaminated sediments in the sediment column.

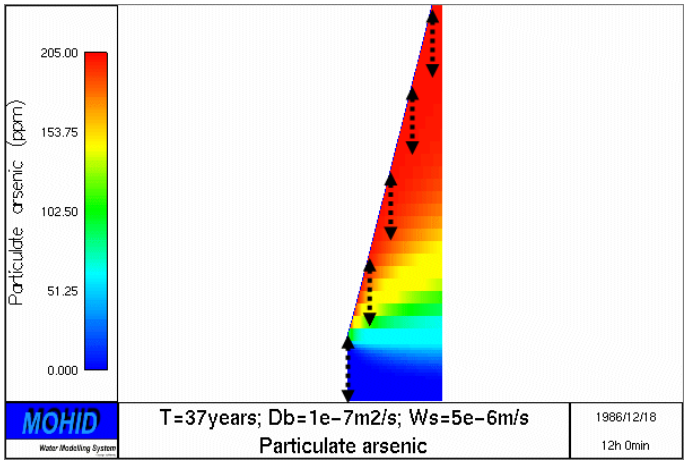

Figure 46 – Contamination scenario; Particulate arsenic concentration profile evolution (Time vs. Depth) during 37 years, with bioturbation coefficient = $10^{-7}m^2/s$ and SPM deposition flux = $5x10^{-4}g/m^2s$; Initial sediment thickness = 20cm

As it can be seen (with guidance provided by the 20cm arrows defining the upper 20cm of the sediment bed, in Figure 46), with high deposition rates, contaminated sediments cover sequentially the underlying layers, and due to bioturbation, high concentrations particulate arsenic can be found deep in the sediment column, ultimately constituting its final destination.

The second scenario was setup assuming no discharge (the plant was shut down around 1986/87) and the model was run from that time until present days. Thus, residual concentrations were considered in the water column, and all parameterizations were maintained in relation to the first scenario. Initial conditions in the sediment compartment were obtained from the contamination scenario. Results are presented for two simulations using a bioturbation coefficient of $10^{-7}m^2/s$ and sedimentation rates of $10^{-5}g/m^2s$ and $5x10^{-4}g/m^2s$.

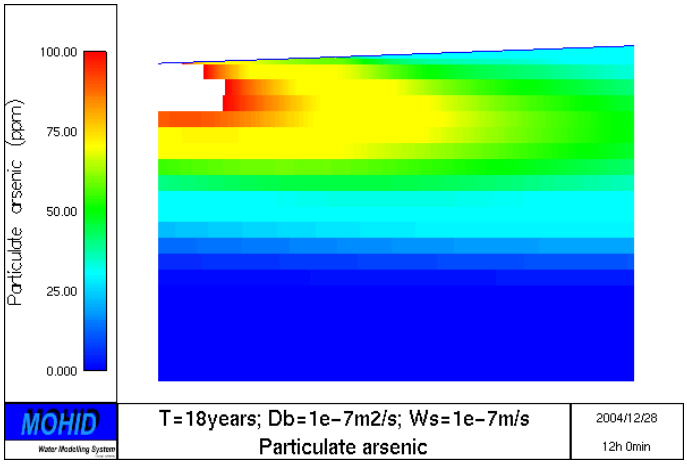

Figure 47 – No discharge scenario; Particulate arsenic concentration profile evolution (Time vs. Depth) during 18 years, with bioturbation coefficient = $10^{-7}m^2/s$ and SPM deposition flux = $10^{-5}g/m^2s$;

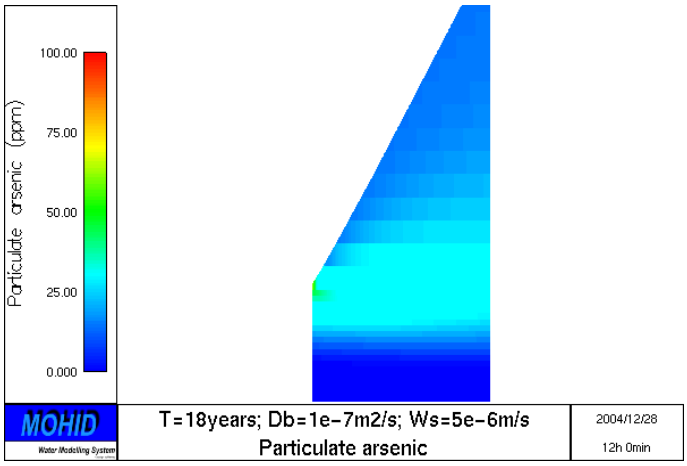

Figure 48 - No discharge scenario; Particulate arsenic concentration profile evolution (Time vs. Depth) during 18 years, with bioturbation coefficient = $10^{-7}m^2/s$ and SPM deposition flux = $5x10^{-5}g/m^2s$;

Results show that high deposition rates of uncontaminated sediments reduce top layer adsorbed sediment concentrations, being the bioturbation effects the responsible factor to mix arsenic in these recent deposits. As it can be seen, if the deposition rate is too high, a layer with relatively high concentration of arsenic will ultimately remain buried, due to the fact that bioturbation mixing effect is only considered until 10cm below sediment surface. Thus, results show that a slow decontamination of the sediment compartment is taking place, being bioturbation and sedimentation rates key processes. Below (Figure 49) shows an interstitial water arsenic profile from the end of the "no discharge" scenario, presented in Figure 47.

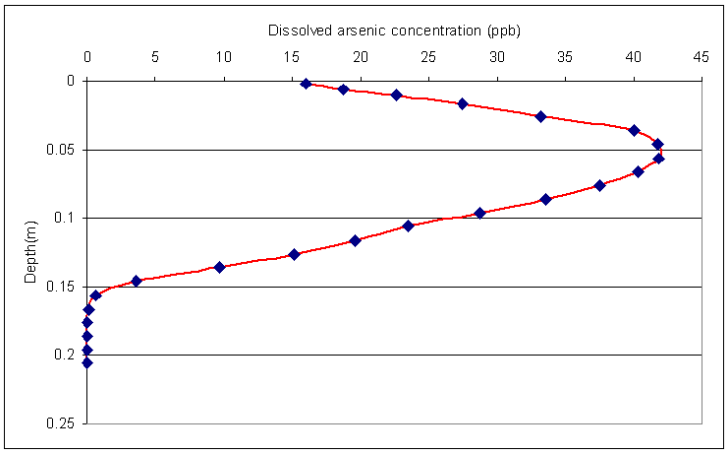

Figure 49 – No discharge scenario; Dissolved arsenic in interstitial water after 18 years simulation with bioturbation coefficient = $10^{-7}m^2/s$ and SPM deposition flux = $10^{-5}g/m^2s$;

The shape of the profile clearly shows the decontamination phase, as lower concentrations are found near the sediment surface, indicating a steep gradient between the water column above and the interstitial water. This gradient, nevertheless, is also controlled by partitioning, as equilibrium concentrations must be respected even if arsenic is leaving the sediment column by diffusion. One has also to keep in mind that, as sedimentation of uncontaminated sediments occurs, adsorbed concentrations become lower in the top layers, therefore reducing equilibrium concentrations of the dissolved phase.

The simulations presented above are sensitivity analysis of the model. Realistic simulations of the Tagus estuary will be performed in the future and conclusions on this study can be drawn with greater detail. Nonetheless, results are satisfactory as they present a good approach of the conceptual model of arsenic dynamics in the Tagus estuary and therefore this technology is available and ready to contribute to further knowledge of the governing processes in this dynamics.

6 CONCLUSIONS

6.1. Model developments

A contaminant transport model was developed and coupled to MOHID Water Modelling System. As described in this thesis, a general review of the software code was performed, resulting in a model restructure, namely through the redefinition of modules hierarchy, in order to enable a consistent description of the environmental compartments to be modelled: sediment, water and atmosphere. This allowed for new developments in environmental modelling, namely through the inclusion of several different models, other than the historic 3D hydrodynamic and transport model, such as: sediment compartment model, a watershed model, river networking, soil water infiltration and aquifer models; as well as it improved the coupling of meteorological models or other types of atmospheric forcing, with the creation of the *Atmosphere* and *InterfaceWaterAir* modules. Polymorphism and code re-use through inheritance are some of the object-oriented (OO) features used in MOHID source code which enabled this step forward in environmental modelling. The models' OO programming philosophy proved to be an important feature in the reorganization task, as it was relatively straightforward. Some new OOP features where included, namely in the way memory and objects are managed during model execution. The overall gain was a more robust and versatile software platform.

The main developments in relation to this study were performed in the sediment compartment, namely through the introduction of a physical processes module handling consolidation and erosion processes, and a transport model to account for the dynamics of sediment properties (namely contaminants) due to the physical and biogeochemical processes occurring there.

6.2. Model results – Calibration

Several test cases were performed to assess model reliability to the newly included processes. Results were useful to calibrate some parameters and refine some approaches, resulting in an overall agreement with the design of the conceptual model.

6.3. Arsenic dynamics in the Tagus estuary

The model was tested and applied in the Tagus estuary with the objective of defining a modelling methodology to study arsenic dynamics in this system, which was subjected to arsenic contamination during several decades. Hydrodynamics and cohesive sediment transport were identified as the processes influencing in the estuarine distribution of contaminants. Model results were validated against measurements and reproduce the overall known dynamics of the Tagus estuary. A new methodology to estimate critical shear stresses for erosion to occur was implemented, which improved the initial condition estimation for the bottom boundary and a good estimation of sediment distribution in the estuary.

Arsenic measurements taken in the Tagus estuary show that arsenic fractions adsorb on to sediment particles can reach up to 80% of the total distribution in the water column. This results in deposited contaminated sediments accumulating in deposition zones, reaching high levels, which can trigger contamination conditions for the benthic and pelagic biotic communities, and ultimately for Man.

Model results have shown to have qualitatively well simulated arsenic distribution, both in the water column and in the sediments, based in measurements taken at the time of the discharges made by the pyrite processing industry. Arsenic vertical distribution in the sediments was simulated and vertical concentration profiles, both for the porewater

dissolved fraction and adsorbed fractions were obtained, providing a good overview of processes controlling the detainment of arsenic in the sediments.

6.4. Future work

A relatively high amount of new processes were included in the model in order to simulate estuarine contaminant transport. Most developments were made in terms of cohesive sediment transport, leaving coarser sediment dynamics to a secondary role, as it is considered that inert sediments such as sand having little affinity with contaminants. Nevertheless, they too are a constitutive part of the sediment compartment and can interfere with the finer fraction by mixing with it, and therefore should also be included in following integrated studies of contaminant transport.

Many of these new processes have not been fully tested for a set of different conditions, but the technology is implemented and available, and will improve with more applications, not only with new parameterizations, as well as correcting possible inconsistencies. This is a common feature in software development.

Full model applications were not performed and long term simulations were not presented in the framework of this study. Nevertheless, this study will continue, and the applications will be performed in order to validate the model in a more qualitative way. The validation of long term modelling simulations will provide the model with the necessary adjustments for it to be used to study arsenic dynamics in the Tagus estuary. Especially now, that the pyrite processing plant was closed and there is no significant anthropogenic input of arsenic into the estuary. It is expected, as seen from preliminary model results that the contaminated sediments, in some areas, will be continuously, and at a slow rate, washed out and ultimately arsenic will be removed from the superficial sediments.

The methodology followed to study contaminant transport can be, in fact, a precursor for another important step to model water quality and ecological processes in estuaries. This is due to the fact that it will be relatively straightforward to include biogeochemical reactions modules to simulate organic matter mineralization in the sediments, and therefore improve the bottom boundary conditions of the pelagic transport and water quality model, used to study and assess eutrophication, one of the major water quality problems, as stated by the European Water Framework Directive.

7 REFERENCES

Allen, C. M.**, 1982,** Numerical simulation of contaminant dispersion in estuary flows, Proc. R. Soc. London. A 381, 179-194

Amos, C. L., Van Wagoner, N. A. & Daborn, G. R., **1988**, The influence of subaerial exposure on the bulk properties of finegrained intertidal sediment from Minas Basin, Bay of Fundy. Estuarine and Coastal Shelf Science, 27, 1–13.

Akin, J. E., **1999**, Object Oriented Programming via FORTRAN 90, Engineering Computations, 16, 1, 26-48

Akin, J. E., **2001**, Object Oriented Programming via FORTRAN 90/95, Cambridge University Press, in press (draft version)

Andreae, M., Byrd, J.T. and Froelich, P.N. Jr, **1983**, Arsenic, Antimony, Germanium, and Tin in the Tejo Estuary, Portugal: Modeling a Polluted Estuary, Environ. Sci. Technol., 17, 731-737

Backhaus, J. O. and Hainbucher, D., **1987**, A finite-difference general circulation model for shelf seas and its application to low frequency variability on the North European Shelf, In: J. C. J. Nihoul and B. M. Jamart (eds.), Three-Dimensional Models of Marine and Estuarine Dynamics, Elsevier Oceanography Series, 45: 221- 244

Bettencourt, A., **1990**, Especiação e biogeoquímica do arsénio no Estuário do Tejo, Dissertação apresentada para a obtenção do grau de Doutor em Ciências do Ambiente (Biogeoquímica Ambiental) pela Universidade de Évora, Évora

Boudreau, B.P., **1996**, The diffusive tortuosity of fine-grained unlithified sediments. Geochimica et Cosmochimica Acta**,** 60**,** 3139-3142

Boudreau, B.P., **1997**, A one dimensional model for bed-boundary layer particle exchange, Journal of Marine Systems, 11, 3-4, 279-303

Braunschweig, F., **2001,** Generalização de um modelo de circulação costeira para albufeiras, Dissertação para a obtenção do grau de Mestre em Ecologia, Gestão e Modelação de Recursos Marinhos, Instituto Superior Técnico, Lisboa

Braunschweig, F., F. Martins, P. C. Leitão, R. Neves, **2003**, A methodology to estimate renewal time scales in estuaries: the Tagus Estuary case, Ocean Dynamics, Volume 53 (3), 137 - 145

Braunschweig, F., P. Chambel, L. Fernandes, P. Pina, R. Neves, **2004a**, The object-oriented design of the integrated modelling system MOHID, Computational Methods in Water Resources International Conference, Chapel Hill, North Carolina, USA

Braunschweig, F., R. Neves, P. Chambel, L. Fernandes, **2004b**, Modelação Integrada de Sistemas Hídricos, 7º Congresso da Água, Associação Portuguesa dos Recursos Hídricos, Lisboa, Portugal

Burchard, H., Bolding, K., and Villarreal, M.R., **1999**, GOTM - a general ocean turbulence model, Theory, applications and test cases, Technical Report EUR 18745 EN, European Commission.

Cancino, L., **Neves**, R., **1999a**, Hydrodynamic and sediment suspension modelling in estuarine systems, Part I: Description of the numerical models, Journal of Marine Systems, 22, 105-116

Cancino, L., **Neves**, R., **1999b**, Hydrodynamic and sediment suspension modelling in estuarine systems, Part II: Application to the Western Scheldt and Gironde estuaries , Journal of Marine Systems, 22, 117-131

Cary, J. R., S. G. Shasharina, J. C. Cummings, J. V. W. Reynders, P. J. Hinker, **1997,** A Comparison of C++ and Fortran 90 for Object-Oriented Scientific Programming, Computer Phys. Comm., 105, 20

Christie, M. C., K. R. Dyer and P. Turner, **1999,** Sediment Flux and Bed Level Measurements from a Macro Tidal Mudflat, Estuarine, Coastal and Shelf Science, 49, 667–688

Coelho, H., Neves, R., White, M., P. C. Leitão, Santos, A., **2002**, A Model for Ocean Circulation on the Iberian Coast, Journal of Marine Systems, 32 (1-3), 153-179

de **Clipelle**, J., Cohesive Sediment Transport in the Tagus Estuary, **1998,** Diplôme d'Etudes Approfondies Européen en Modélisation de L'Environment, Erasmus

Decyk, V. K, C. D Norton, B. K. Szymanski, **1997a**, Introduction to Object-Oriented Concepts using Fortran90, Unpublished

Decyk, V. K., C. D. Norton, B. K. Szymanski, **1997b**, Expressing Object-Oriented Concepts in Fortran90, ACM Fortran Forum, 16

Decyk, V. K, C. D Norton, B. K. Szymanski, **1998,** How to Support Inheritance and Run-Time Polymorphism in FORTRAN 90, Computer Physics Communications, 115, 9-17

EUROSSAM, **2000** – Task 8 Modelling the Biogeochemical Processing of Arsenic by Salt Marshes, Final Report, Institute of Marine Research, Biogeochemistry Group, Évora, Portugal

Fabian, D., Zhou, Z., Wehrli, B. Friedl, G., **2003**, Diagenetic cycling of arsenic in the sediments of eutrophic Baldeggersee, Switzerland

Garcia, A.C., **1997**, Dispersão e deposição da matéria particulada transportada em suspensão para a plataforma continental adjacente aos Rios Tejo e Sado, Dissertação para obtenção do grau de Mestre em Geologia, Faculdade de Ciências da Universidade de Lisboa, Lisboa

Graf, G., R. **Rosenberg**, **1997**, Bioresuspension and biodeposition: a review, Journal of Marine Systems, 11, 3-4, 269-278

Gray, M.G., and **Roberts**, R.M., **1997**, "Object-Based Programming in Fortran 90", Computers in Physics, 11, 355

Hayter, E. J., C.V. **Pakala**, **1989,** Transport of inorganic contaminants in estuarial waters, Journal of Coastal Research, Special Issue 5, 217-230

Hayter, Earl J., Mary A. Bergs, Ruochuan Gu,Steve C. McCutcheon, S. Jarrell Smith, and Holly J. Whiteley, **1995**, HSCTM-2D, A finite element model for depth averaged hydrodynamics, sediment and contaminant transport, User manual

Houwing, E.-J., **1999,** Determination of the critical erosion threshold of cohesive sediments on intertidal mudflats along the Dutch Wadden Sea Coast, 49, 545-555

INAG (Instituto da Água) / MARETEC, **2002**, Water Quality in Portuguese Estuaries: Tejo, Sado and Mondego, Lisbon

J. **Smagorinsky**, **1963**, General circulation experiments with the primitive equations, Monthly Weather, Review, 91(3), 99–165.

James, I.D., **2002,** Modelling pollution dispersion, the ecosystem and water quality in coastal waters: a review, Environmental Modelling & Software, 17, 363-385

Johasson, H., Lindstrom, M., Hakanson, L., **2001**, On the Modelling of particulate and dissolved fractions of substances in aquatic systems – sedimentological and ecological interactions, Ecological Modelling, 137, 225-240

Krone, R., **1962**, Flume Studies of the Transport in Estuaries Shoaling Processes, Hydr. Eng. Lab., University of Berkeley, California, USA

Le Provost, C., F. Lyard, J.M. Molines, M.L. Genco and F. Rabilloud, **1998**, A Hydrodynamic Ocean Tide Model Improved by assimilating a satellite altimeter derived dataset. J. Geophys. Res. Vol., 103 N. C3, 1998.

Leendertse, J. J. and **Liu**, S. K., **1978**: A Three-dimensional turbulent energy model for non-homogeneous estuaries and coastal sea systems. Hydrodynamics of Estuaries and Fjords, J.C.J. Nihoul Ed., Elsevier Publ. Co., Amsterdam, pp. 387-405.

Leitão, P., **2003**, Integração de Escalas e Processos na Modelação do Ambiente Marinho, Dissertação para a obtenção do grau de Doutor em Engenharia do Ambiente, Instituto Superior Técnico, Lisboa

Leitão, P.C., **1996,** Modelo de dispersão lagrangeano tridimensional, Dissertação para a obtenção do grau de Mestre em Ecologia, Gestão e Modelação de Recursos Marinhos, Instituto Superior Técnico, Lisboa

Linde, K., **2002,** Assessment of Contaminant Availability in a Shallow Wetland, PhD thesis in Environmental Chemistry, University of Western Australia, Centre for Water Research

Martin, J.M., Figuéres, G., Meybeck, M., **1982**, Etude de l'environnement de l'estuaire du Tage, Le mercure et l'arsenic dans l'estuaire du Tage, Comissão Nacional do Ambiente, Lisboa

Martino, M., A. Turner, M. Nimmo, G. E. Millward, **2002**, Resuspension, reactivity and recycling of trace metals in the Mersey Estuary, UK, Marine Chemistry, 77, 171-186

Martins, F. **2000**, Modelação Matemática Tridimensional de Escoamentos Costeiros e Estuarinos usando uma Abordagem de Coordenada Vertical Genérica, Dissertação para obtenção do grau de Doutor em Engenharia Mecânica, Instituto Superior Técnico, Universidade Técnica de Lisboa

Martins, F., P. C. Leitão, A. Silva, R. Neves, **2001**, 3D modelling of the Sado Estuary using a new generic vertical discretization approach, Oceanologica Acta, 24 (1), 51-62

McAnnaly, W. H., **Mehta**, A. J., **2001,** Collisional aggregation of fine estuarial sediment, Coastal and Estuarine Fine Sediment Processes, McAnnaly, W. H., Mehta, A. J. (Editors), Elsevier Science B. V., Proceedings in Marine Science 3, 19-39

Mehta, A. J., **1988,** Laboratory Studies on Cohesive Sediment Deposition and Erosion, Physical Processes in Estuaries, Springer-Verlag, Berlin Heidelberg New York, Job Dronkers and Wim van Leussen (Editors)

Mellor, G. L. and **Yamada**, T., **1982**: Development of a turbulence closure model for geophysical fluid problems. *Rev. Geophys. Space Phys.*, **20**, 851-875.

Millward, G. E., Y. P. **Liu**, **2003,** Modelling metal desorption kinetics in estuaries, the Science of Total Environment, 314-316, 613-623

Miranda, R., **1999**, Nitrogen Biogeochemical Cycle Modeling in the North Atlantic Ocean, Dissertação para a obtenção do grau de Mestre em Ecologia, Gestão e Modelação de Recursos Marinhos, Instituto Superior Técnico, Lisboa

Miranda, R., F. Braunschweig, P. Leitão, R. Neves, F. Martins, A. Santos, **2000,** MOHID 2000, A Coastal integrated object oriented model. Hydraulic Engineering Software VIII, WIT Press

Monteiro, P. M. S., S. Luger, P. J. Pretorius, R. Van Ballegooyen, **1999,** Simulation of eutrophication and particle dynamics in a bay system in order to predict the transport and fate of trace metals using the Delft3D-Flow and –WAQ models, Conference Paper at Proceedings of Pollution, Lemnos, Greece, May 1999

Neves, R. J. J., **1985,** Étude Expérimentale et Modélisation des Circulations Transitoire et Résiduelle dans l'Estuaire du Sado. Ph. D. Thesis, Univ. Liège

Nihoul, J.C.J., **1984**, A three-dimensional general marine circulation model in a remote sensing perspective, In Annales Geophysicae, 2, 4, 433-442

Pacanowski, R. C. and G. H. Philander, **1981**, Parameterization of vertical mixing in numerical models of tropical oceans, J. Phys. Oceanogr., 11, 1443-1451,

Partheniades, E., **1965**, Erosion and Deposition of Cohesive Soils, J. Hydr. Div., ASCE, 91 (1), 105-139

Pina, P., **2001,** Integrated Approach to Study the Tagus Estuary Water Quality, Dissertação para a obtenção do grau de Mestre em Ecologia, Gestão e Modelação de Recursos Marinhos, Instituto Superior Técnico, Lisboa

Pina, P., Saraiva, S., Fernandes, L., Frank Braunchweig, Chambel P. C., and Neves, R., Modelling estuarine systems: the Tagus application, **2004**, Hydrobiologia (submitted), Lisboa

Portela, L., **1996**, Modelação Matemática de Processos Hidrodinâmicos e de Qualidade da Água no Estuário do Tejo, Dissertação para obtenção do grau de Doutor em Engenharia do Ambiente, Instituto Superior Técnico, Universidade Técnica de Lisboa

Portela, L., **1997,** Comportamento de sedimentos contaminados em meio estuarino, Prova Complementar de Doutoramento em Engenharia do Ambiente, Instituto Superior Técnico, Lisboa

Riedel, G. F., **1993,** The Annual Cycle of Arsenic in a Temperate Estuary, Estuaries, 16, 3A, 533-540

Riedel, G. F., Sanders, J. G., Osman, R. W., **1997,** Biogeochemical Control on the Flux of Trace Elements from Estuarine Sediments: Water Column Oxygen Concentrations and Benthic Infauna, Estuarine, Coastal and Shelf Science, 44, 23-3

Rumbaugh, J., M. Blaha, W. Premmerlani, F. Eddy, W. Lorensen, **1991,** Object-oriented modeling and design, Prentice Hall International Editions, USA

Sanders, J. G., Riedel, G. F., Osman, R. W., **1994,** Arsenic Cycling and Its Impact In Estuarine and Coastal Marine Ecosystems, Technical Reprint, University of Maryland, Arsenic in the Environment, Part I: Cycling and Characterization, Edited by Jerome O. Nriagu, John Wiley & Sons, Inc.

Santos, A. J., 1995, Modelo Hidrodinâmico Tridimensional de Circulação Oceânica e Estuarina, Dissertação para obtenção do grau de Doutor em Engenharia Mecânica, Instituto Superior Técnico, Universidade Técnica de Lisboa

Santos, A., H. Martins, H. Coelho, R.Neves, P. C. Leitão, **2002**, A circulation model for the European ocean margin, Applied Mathematical Modelling, 26(5), 563-582

Saraiva, S., Pina, P., Martins, F., Santos, M., Braunschweig, F., Neves, R., **2004**, EU-Water Framework: dealing with nutrients loads in Portuguese estuaries, Hydrobiologia (submitted)

Silva, A., P. C. Leitão, J. C. Leitão, F. Braunschweig, R. Neves, **2002**, Ria Formosa 3D hydrodynamic model. A contribution for the understanding of the Faro-Olhão inlet processes, Littoral 2002, Porto, Portugal

Trancoso, A., Saraiva, S., Fernandes, L., Pina, P., Leitão, P. and Neves, R., **2005**, *Modelling Macroalgae using a 3D hydrodynamic ecological model in a shallow, temperate estuary*, Ecological Modelling (in press)

Turner, A. & **Millward**, G. E., **2002,** Suspended particles: their role in estuarine biogeochemical cycles, Estuarine, Coastal and Shelf Science, 55, 857-883

UNESCO, 1981, Tenth Report on the joint panel on oceanographic tables and standards, Technical papers in marine science, N. 36, 24 pp

Van der Lee, W. T .B., **2001,** Parameters affecting mud floc size on a seasonal time scale: The impact of a phytoplankton bloom in the Dollard estuary, The Netherlands, Coastal and Estuarine Fine Sediment Processes, McAnnaly, W. H. & Mehta, A. J (Editors), Elsevier Science B. V., Proceedings in Marine Science 3, 403-421

Van Vliet, H., **2000,** Software Engineering – Principles and Practice, 2nd Edition, John Wiley & Sons, Ltd, England

Villarreal, M. R., P. Montero, J. J. Tabuada, R. Prego, P. C. Leitão, V. Pérez-Villar, **2002**, Hydrodynamic model study of the Ria de Pontevedra under estuarine conditions, Estuarine, Coastal and Shelf Science, 54, 101-113

Walker, C. H., Hopkin S. P., Sibly R. M., Peakall D. B., **1996,** Principles of ecotoxicology, Taylor & Francis Publishers, London, UK

Winterwerp, J. C., **2002,** On the flocculation and settling velocity of estuarine mud, Continental Shelf Research, 22, 1339-1360